

ISTANBUL TECHNICAL UNIVERSITY ★ GRADUATE SCHOOL OF SCIENCE
ENGINEERING AND TECHNOLOGY

**THE EFFECT OF LIPOSOME PHOSPHOLIPID CONTENT ON THE
FORMATION OF TETHERED LIPID MEMBRANES**

M.Sc. THESIS

Başak TÜRKEN

Department of Advanced Technologies

Molecular Biology & Genetics and Biotechnology Programme

JUNE 2012

ISTANBUL TECHNICAL UNIVERSITY ★ GRADUATE SCHOOL OF SCIENCE
ENGINEERING AND TECHNOLOGY

**THE EFFECT OF LIPOSOME PHOSPHOLIPID CONTENT ON THE
FORMATION OF TETHERED LIPID MEMBRANES**

M.Sc. THESIS

Başak TÜRKEN
(521091082)

Department of Advanced Technologies

Molecular Biology & Genetics and Biotechnology Programme

Thesis Advisor: Assist. Prof. Dr. Fatma Neşe KÖK

JUNE 2012

İSTANBUL TEKNİK ÜNİVERSİTESİ ★ FEN BİLİMLERİ ENSTİTÜSÜ

**LİPOZOM FOSFOLİPID İÇERİĞİNİN YÜZEYE BAĞLI YAPAY LİPİT
MEMBRAN MODELİNİN OLUŞUMU ÜZERİNDEKİ ETKİSİ**

YÜKSEK LİSANS TEZİ

**Başak TÜRKEN
(521091082)**

İleri Teknolojiler Anabilim Dalı

Moleküler Biyoloji & Genetik ve Biyoteknoloji Programı

Tez Danışmanı: Yard. Doç. Dr. Fatma Neşe KÖK

HAZİRAN 2012

Başak TÜRKEN, a M.Sc. student of ITU **Graduate School of Science Engineering and Technology**, student ID **521091082**, successfully defended the thesis entitled “**THE EFFECT OF LIPOSOME PHOSPHOLIPID CONTENT ON THE FORMATION OF TETHERED LIPID MEMBRANES**”, which she prepared after fulfilling the requirements specified in the associated legislations, before the jury whose signatures are below.

Thesis Advisor : **Assist. Prof. Dr. Fatma Neşe KÖK**
Istanbul Technical University

Jury Members : **Assoc. Prof. Dr. Ayten YAZGAN KARATAS**
Istanbul Technical University

Assoc. Prof. Dr. Özgür ÖZER
Istanbul Technical University

Date of Submission : 4 May 2012
Date of Defense : 5 June 2012

Know thyself,

FOREWORD

First, I would like to thank my cheerful supervisor Assist. Prof. Dr. Fatma Neş e KÖK for her guidance. I am indebted her for giving me the chance in her research group.

I am grateful for guidance to Fatih İNCİ who has been helpful and friendly to me, for sharing his knowledge. I would also like to kindly thank to all members of our group and my labfriends.

On a personal note, I want to say “thank you” to my beloved family for their love, belief in me and understanding.

This study was supported by TUBITAK under Grant No.TBAG-108T933 and ITU-BAP Project (34068).

June 2012

Başak TÜRKEN
Molecular Biology and Genetics

TABLE OF CONTENTS

	<u>Page</u>
FOREWORD	ix
TABLE OF CONTENTS	xi
ABBREVIATIONS	xiii
LIST OF TABLES	xv
LIST OF FIGURES	xvii
SUMMARY	xix
ÖZET	xxi
1. INTRODUCTION	1
1.1 .Purpose of Thesis	2
2. BACKGROUND INFORMATION	3
2.1 Lipids.....	3
2.2 Phospholipids	5
2.3 Biomimetic Model Membrane Systems	7
2.4 Surface Plasmon Resonance (SPR).....	10
2.4.1 Principle of SPR.....	12
2.5 Quartz Crystal Microbalance with Dissipation (QCM-D).....	12
2.5.1 Basic principle of QCM-D.....	13
2.5.2 The dissipation.....	14
3. MATERIALS AND METHODS	17
3.1 Material	17
3.2 Equipments.....	17
3.2.1 Surface plasmon resonance (SPR)	17
3.2.1.1 Preparation of SPR set-up	18
3.2.2 Quartz crystal microbalance with dissipation monitoring (QCM-D)	18
3.2.2.1 Preparation of QCM-D set-up.....	19
3.3 Construction of Tethered Bilayer Lipid Membranes (tBLMs)	19
3.3.1 Functionalization of the gold films	20
3.3.2 Construction of DSPE-PEG as a second layer.....	20
3.3.3 Preparation of liposomes and construction of tBLMs as a third layer	21
4. RESULTS & DISCUSSION	23
4.1 Effect of membrane composition	23
4.1.1 Formation of DSPE-PEG monolayer	24
4.1.2 The effects of percentage of PE on PC/PE liposomes	25
4.1.3 The effects of percentage of PS on PC/PS liposomes.....	29
4.2 Effect of Liposome Size	34
5. CONCLUSIONS AND RECOMMENDATIONS	35
REFERENCES	37
APPENDICES	41
APPENDIX A.....	42
APPENDIX B.....	43

CURRICULUM VITAE 45

ABBREVIATIONS

AFM	: Atomic Force Microscopy
BLMs	: Black lipid membranes
D	: dissipation
DMSO	: dimethyl sulfoxide
DSPE-PEG	: 1,2-distearoyl-sn-glycero-3-phosphoethanolamine-N-[amino (polyethylene glycol)-2000
DTSP	: 3,3'-Dithiodipropionic acid di(N-hydroxysuccinimide)
f	: resonance frequency (Hz)
PBS	: phosphate buffered saline
PE	: phosphatidylethanolamine
PC	: phosphatidylcholine
PS	: phosphatidylserine
RIU	: refractive index unit
QCM-D	: quartz crystal microbalance with dissipation monitoring
SPR	: surface plasmon resonance
SLBs	: solid supported lipid bilayers
tBLMs	: tethered lipid bilayers

LIST OF TABLES

	<u>Page</u>
Table 3.1 : Different lipid compositions.....	21

LIST OF FIGURES

	<u>Page</u>
Figure 2.1 : Packing arrangements of lipid molecules in an aqueous environment...	3
Figure 2.2 : Classification of lipids.....	4
Figure 2.3 : A drawing of a small spherical liposome seen in cross section.....	4
Figure 2.4 : A cross-sectional view of a black membrane, a synthetic lipid bilayer...	5
Figure 2.5 : The chemical structures of phosphatidylserine (PtdSer), phosphatidylethanolamine (PtdEtn) and phosphatidylcholine (PtdCho)..	6
Figure 2.6 : Models of biological membranes.	8
Figure 2.7 : Main Application areas of SPR Technology.....	11
Figure 2.8 : Schematic illustration of SPR Phenomena.	12
Figure 2.9 : A Sensogram.	13
Figure 2.10 : Schematic illustration of AT-cut quartz crystal.....	14
Figure 2.11 : Example of raw data from a QCM-D experiment.	15
Figure 3.1 : SR7000 Single Channel Surface Plasmon Resonance Spectrometer	17
Figure 3.2 : The fully assembled QCM and the electronic unit.	18
Figure 3.3 : The insertion of o-ring and quartz crystals.....	19
Figure 3.4 : Structural formula of DTSP.	19
Figure 3.5 : Structural formula of DSPE-PEG.	19
Figure 3.6 : This figure illustrates construction of tBLMs layer on the gold surface.	20
Figure 3.7 : The whole extruder system.....	22
Figure 4.1 : Change in SPR refractive index (A) and QCM-D frequency (B) versus time demonstrating the interaction of DSPE-PEG with DTSP covered gold surface to form the second layer.	24
Figure 4.2 : Change in SPR refractive index versus time for the interaction of PC and PC/PE liposomes onto the gold surface as a third layer.	26
Figure 4.3 : Change in QCM resonant (normalized) frequency and dissipation versus time for the interaction of PC liposomes onto the gold surface.....	27
Figure 4.4 : Change in QCM resonant (normalized) frequency and dissipation versus time for the interaction of 75PC/25PE liposomes onto the gold surface.	28
Figure 4.5 : Change in QCM resonant (normalized) frequency and dissipation versus time for the interaction of PE liposomes onto the gold surface.....	28
Figure 4.6 : Change in SPR refractive index versus time for the interaction of PC and PC/PS liposomes onto the gold surface.	30
Figure 4.7 : The evanescent field of SPR.	30
Figure 4.8 : Change in QCM resonant frequency (normalized) and dissipation versus time for the interaction of 75PC/25PS liposomes onto the gold surface.	31
Figure 4.9 : Change in QCM resonant frequency (normalized) and dissipation versus time for the interaction of PS liposomes onto the gold surface.	32

Figure 4.10 : SPR sensogram of 25PC/75PS liposomes rinsed by 70% of ethanol solution.....	33
Figure 4.11 : Change in SPR refractive index versus time for the interaction of PC/PE liposomes, which are formed by 50nm membrane, onto the gold surface.	34

THE EFFECT OF LIPOSOME PHOSPHOLIPID CONTENT ON THE FORMATION OF TETHERED LIPID MEMBRANES

SUMMARY

Biological membranes are vital structures for cell life. Because of the complexity of biological membranes, it is very important to develop model membrane systems to study membrane components.

Tethered lipid bilayer membranes (tBLMs) on planar surfaces provide an important media to mimic the lipid bilayer membrane in vitro. tBLMs can be used for applications such as biosensors or as a model system to study the structure and function of biomembranes and membrane proteins. Techniques such as surface plasmon resonance (SPR) and quartz crystal microbalance with dissipation (QCM-D) provide important information about adsorption kinetics of liposomes on the surface by using refractive index and dissipation (ΔD) -and frequency (Δf) change values. In addition, ΔD and Δf values allow determining viscoelastic properties of lipid components on the surface.

In this work, the properties of tethered lipid bilayer membranes (tBLMs) constructed by different phospholipids (saturated phosphatidylcholine (PC), phosphatidylethanolamine (PE) and phosphatidylserine (PS)) were studied and the whole process was followed by SPR. Lipid composition is expected to affect the bilayer properties like viscoelastic properties. This characteristic was determined by the help of QCM-D. tBLMs were formed according to the procedure optimized in our group. In order to construct tBLMs, either SPR gold covered slides or QCM gold covered crystals were activated with 3, 3'-dithiodipropionic acid di(N-hydroxy succinimide ester) (DTSP) dissolved in dimethyl sulfoxide (DMSO, 1mM). DTSP self-assembled on Au surfaces via its thiol groups. 1,2-distearoyl-sn-glycero-3-phosphoethanolamine-N-[amino poly ethyleneglycol)-2000] (DSPE-PEG) was then incubated with DTSP covered surfaces to form second layer on the surface and it was attached on it to serve as tethers for the tBLMs. To construct final layer, liposomes with different composition and different compounds (PC/PE and PC/PS: 90:10, 25:75, 50:50 and vice versa) were produced by the help of an extruder using 100 nm membranes and spread over the modified surface.

PC/PE liposomes showed higher refractive index and ΔD and Δf values than PC liposomes. This states that, increasing PE concentration affects membrane fluidity and led liposomes to stably attach to the surface without forming bilayer, whereas bilayer formation was more favored in lower PE ratios.

Likewise, adding PS to PC liposomes caused the formation of intact multi-vesicles layer on the surface. This can be predicted from SPR and QCM-D results, because refractive index value of PC/PS liposomes was significantly higher than PC and PC/PE liposomes and ΔD and Δf values increased by adding more PS to PC liposomes. There was no change in frequency values even after rinsing. In addition,

70% of ethanol solution was used to trigger vesicle fusion on 25PC/75PS liposomes. Unfortunately, the whole unattached lipids were washed off from the system at this concentration.

Additionally, the effect of vesicle size on the formation of tBLMs was investigated. For this, 50 nm diameter of liposomes (90PC/10PE and 75PC/25PE) were prepared. Decreasing vesicle size from 100 nm to 50 nm affected vesicle adsorption to the surface negatively.

In conclusion, the phospholipid content of liposomes have a great impact on the behavior of liposomes and different parameters like the size, fluidity and interaction with different ions affect this behavior. Since the cell membrane of different tissues have different compositions, these parameters should be investigated in more detail.

LİPOZOM FOSFOLİPID İÇERİĞİNİN YÜZEYE BAĞLI YAPAY LİPİT MEMBRAN MODELİNİN OLUŞUMU ÜZERİNDEKİ ETKİSİ

ÖZET

Biyolojik membranlar, oldukça karmaşık ve dinamik yapısıyla, hücre canlılığının çok önemli bir bileşenidir. Hücre canlılığının ve özgün hücre işlevlerinin sürekliliğini mümkün kılan çok önemli bazı fonksiyonları yerine getirir. Karmaşık yapılarından dolayı, farklı membran bileşiklerinin çalışılabilmesi için yeni yapay lipit membran modellerinin geliştirilmesi çok önemlidir.

Katı bir yüzeye bağlı lipit membran modeli (tBLMs), çift katmanlı lipit membranların taklit edilmesi için uygun bir ortam sağlar. Bu yapay lipit membran modelinde, çift katmanlı lipit membran yüzeyden hidrofilik bir ara tutucu molekülle ayrılır. Böylece lipit membranın katı yüzeyden etkilenmesi ve stabilitesinin artması amaçlanır. tBLMs, biyosensör uygulamaları veya biyomembranların ve membran proteinlerinin yapı ve fonksiyonlarının araştırılmasında kullanılan bir yapay lipit membran modelidir.

Memeli hücre membranları 1000 değişik fosfolipid çeşidi içerir. Bu kadar çeşitli fosfolipid miktarı, membranın akışkanlığını ve membrana gömülü olan proteinlerin işlevlerini belirler. Bir çok memeli hücrenin plazma membranında, fosfatidilkolin (PC), fosfatidiletanolamin (PE) ve fosfatidilserin (PS) en çok bulunan fosfolipitlerdir. Bunlardan sadece PS negatif yük taşır, diğer ikisi fizyolojik pH'ta elektriksel olarak nötr haldedir: bir negatif bir de pozitif yük taşırlar (zwitteriyonik).

Fosfatidilkolin (PC), en çok bulunan fosfolipid çeşididir ve memeli hücre membranlarının %40-50'sini oluşturur. PC, primer hücre membran bileşiklerinin üretilmesinde rol oynar, aynı zamanda asetilkolin sentezindeki başlıca bileşendir. Fosfatidiletanolamin (PE), ikinci en sık bulunan fosfolipid çeşididir ve memeli hücre membranlarının %20-50'sini oluşturur. PE, membranlarda çok sayıda yapısal rol oynar. Fosfatidilserin (PS), nicel olarak az sayıda bulunur ve memeli hücre membranlarının %2-10'unu oluşturur. PS, sinir sistemi ve görme duyusunun oluşumunda çok önemli rol oynar. Ayrıca, programlı hücre ölümünde (apoptoz) kullanılan bileşenlerden biridir. Normalde, sitosolik plazma membranında hapsedilmiş olarak bulunan fosfatidilserin, apoptoz esnasında hücre dışı tek katmanına yer değiştirir. Hücre yüzeyinde açıkta kalan PS, çevredeki makrofaj gibi hücrelere sinyal gönderir ve bu şekilde hücrenin parçalanmasına katkıda bulunur.

Yüzey plasmon rezonans (SPR), moleküller arası etkileşimlerin araştırılmasında ve kimyasal ve biyolojik analitlerin tespit edilmesinde kullanılan optik bir cihazdır. SPR cihazının çalışma prensibinin temeli olan polarize ışık, yüzeyi altın kaplı bir prizmaya gönderildiğinde ışığın bir kısmı absorplanmakta, bir kısmı da yansımaktadır. Yansıyan ışığın şiddetinde maksimum kaybın gerçekleştiği açıya rezonans açısı denir. Metal yüzeyiyle temas halinde ortamın özelliklerinin değişmesi

veya yüzeyde madde birikimi olması durumunda rezonans açısı değişmekte ve bu değişiklik yüzeyde olan değişikliklerin anlaşılmasında kullanılabilir.

Kuvars kristal mikroterazi (QCM-D), kütleli değişiklikleri, bir elektrik sinyaline çevirebilen çok kullanışlı bir yaklaşımdır. QCM-D cihazının bünyesinde bulunan kuvars kristalin piezoelektrik özelliği çalışma prensibinin temelidir. Piezoelektrik etki, asimetrik bir kristalin elektrik potansiyelinin uygulanmasıyla deformasyona uğramasıdır. Kuvars kristaller mekanik olarak deforme olduğunda, yüzeyinde elektiriksel bir potansiyel oluşur ve uygun bir elektrik devresine bağlanırsa kristalin kütleline ve şekline bağlı olan sabit bir frekansta titreşim yapar. Yüzeydeki kütle değişimleri, rezonans frekansındaki sapmaya dönüştürülerek yorumlanır. Rezonans frekansına ek olarak, yüzeye bağlanan katmanların viskoelastik özellikleri, enerji yitimi (D) parametresiyle ölçülür. ΔD değerindeki artış yüzeyde viskoelastisitesi yüksek analitlerin bulunduğunu; bu değerdeki düşme ise yüzeyde daha katı (rijit) bir yapının oluştuğunu gösterir.

Bu çalışmada, farklı kompozisyonlarda ve farklı konsantrasyonlarda lipozomlar üretilerek katı bir yüzeye bağlı lipit zar modeli (tBLMs) oluşturuldu ve yüzeye tutunum kinetiklerinin belirlenmesi için yüzey plazmon rezonans (SPR) ve kuvars kristal mikroterazi (QCM-D) yöntemleri kullanıldı. Lipozomları oluştururken 3 farklı fosfolipit molekülü kullanıldı (fosfatidilkolin (PC), fosfatidiletanolamin (PE) ve fosfatidilserin (PS)). Lipit kompozisyonunun, çift katmanlı lipit membranın viskoelastik özelliklerini etkileyeceği düşünüldü ve bu özellik QCM-D cihazı ile tanımlandı. tBLMs, çalışma grubumuzun optimize ettiği prosedüre göre oluşturuldu. Buna göre; altın kaplı SPR ve QCM yüzeyleri dimetil sülfoksitte (DMSO) çözülmüş 3, 3'-dithiodipropionic acid di(N-hydroxy succinimide ester) (DTSP) molekülü ile aktive edildi (DMSO 1mM). DTSP, altın yüzeye tiyol grubu ile kendi kendine bağlanan bir moleküldür ve sistemimizin birinci katmanını oluşturur. İkinci katmanın oluşturulmasında; fosfat kafasına polietilenglikol bağlanmış ve bu uçta bir amino grubu taşıyan bir fosfolipit molekülü (DSPE-PEG), DTSP kaplı yüzey ile inkübe edildi. Bu molekül, tBLMs ile yüzey arasına bir mesafe konulması amacı ile kullanıldı. Üçüncü ve son katman, farklı kompozisyonlarda ve farklı konsantrasyonlarda lipozomların yüzeye gönderilmesiyle oluşturuldu. Lipozomlar zwitteriyonik (çift kutuplu) (PC/PE) ve anyonik yapıda (PC/PS) ve farklı konsantrasyonlarda (90:10, 75:25, 50:50 ve tam tersi) olmak üzere, 100 nm gözenekli membranlar kullanılarak ekstrüzyon yöntemiyle oluşturuldu.

İlk olarak, çalışma grubumuz tarafından adsorbsiyon kinetiği ve tBLMs oluşumu daha önce gözlenen PC lipozomların tBLMs oluşumuna etkisi gözlemlendi. Daha sonra, elde edilen veriler PC/PE ve PC/PS lipozomlarının tBLMs oluşumu üzerindeki etkisinin araştırılması için referans olarak kullanıldı.

Zwitteriyonik PC/PE lipozomların araştırılması sırasında, PC lipozomlar ile karşılaştırıldığında daha yüksek refraktif indeks artışı gözlemlendi. Elde edilen verilerin daha iyi yorumlanabilmesi için ayrıca QCM-D analizleri ile bütünleştirildi. 75PC/25PE ve PE lipozomlardan alınan QCM sonuçlarına göre, PE konsantrasyonu arttıkça ΔD değerinde artış ve Δf değerinde düşüş gözlemlendi. Bu sonuçlar gösteriyor ki, artan PE konsantrasyonu lipozomların yüzeyde bozulmadan kalmasına yolaçmaktadır. Ayrıca, çift katman oluşumu daha düşük PE konsantrasyonunda daha avantajlıdır.

Anyonik PC/PS lipozomların tBLMs oluşumu üzerindeki etkisi incelendiğinde, PC lipozomlara göre oldukça yüksek refraktif index değerlerinin alındığı görüldü. Buna

ek olarak, 75PC/25PS ve PS lipozomların QCM-D tekniđi ile ölçümleri gerçekleştirildi. QCM-D sonuçlarına göre, lipozom içeriğindeki PS miktarı arttıkça büyük miktarlarda ΔD değeriinde artış ve Δf değeriinde düşüş olduđu görüldü. Buna ek olarak, yüzeyde bağlanmadan kalan lipid moleküllerinin uzaklaştırılması için yapılan yıkama sonrasında Δf ve ΔD sinyallerinde deđişim olmadığı gözlemlendi. Yıkama sırasında frekanstaki artma lipozomların yüzeye yayıldığını ve içinde hapsolan suyun sistemden uzaklaştığını göstermektedir. Bu durumda, yıkama sonrasında frekansta deđişimin olmaması ve Δf - ΔD değerlerinin beklenenden çok yüksek olması, lipozomların yüzeyde bozulmadan kaldığını belirtir.

PC/PS lipozomların yüzeye yayılmasını ve tBLMs oluşumunu tetiklemek amacıyla yıkama sonrasında yüzeye % 70 etanol çözeltisi gönderildi ve etkisi SPR ile gözlemlendi. Fakat bu koşullarda yüzeydeki lipozomların tamamen yıkanmadığı gözlemlendi.

Lipozom içeriğinden farklı olarak ayrıca lipozom boyutunun sistem üzerindeki etkisi de SPR cihazı kullanılarak incelendi. Bunun için, 50 nm çaplı 90PC/10PE ve 75PC/25PE lipozomlar kullanıldı. Sonuç olarak, her iki konsantrasyonda da lipozomların yüzeye gönderildiği sırada refraktif indekste artış olduđu, fakat daha sonra yıkama yapılmamasına rağmen refraktif indeksin ilk baştaki değere düştüğü gözlemlendi. Lipozom boyutunun yarıya düşürülmesinin lipozomların yüzeye etkileşmesine rağmen bu etkileşimin çok kararlı olmamasına ve büyük ihtimalle elastisitesi daha az olan bu lipozomların yüzeye yayılmayarak hızla yıkanmasına yol açtığı düşünöldü .

1. INTRODUCTION

Biological membranes play key roles in cell life. They control the transfer of information and the transport of ions and molecules between the inside and outside cellular worlds and participate in various intra- and extracellular processes [1].

Because of the complexity of the biological membranes, their direct investigation is limited at the nanoscale. Lipid bilayer membranes have been developed as a model of biological membranes to allow the interaction and insertion of peptides and membrane proteins in a functional manner [2].

Successful construction of artificial membrane systems would not only improve our understanding of basic cellular functions but also allow us to develop biotechnological tools, biomedical devices, or biofunctional materials. To do this, it is important to develop reliable methods to control the formation of solid supported lipid membranes and to find effective ways to incorporate, and address biological entities, from molecules to cells [1].

The spreading of small lipid vesicles on hydrophilic solid supports presents an attractive and simple route to form supported lipid bilayers (SLBs) [3]. Solid-supported lipid membranes were developed in the recent decade, starting from bilayers floating freely on top of a quartz, indium tin oxide, or gold surface, to polymer-supported and tethered bilayer lipid membranes (tBLMs) [4].

There are various surface sensitive techniques to characterize these systems. The immobilization of the membrane at a surface permits rapid exchange of the fluids in contact with the membrane. It allows the application of surface-sensitive probes such as surface plasmon resonance (SPR), total internal reflection fluorescence microscopy (TIRFM), impedance spectroscopy, and acoustic sensors such as the quartz crystal microbalance (QCM) and surface acoustic wave (SAW) devices [5].

Techniques based on surface plasmons such as Surface Plasmon Resonance (SPR), SPR Imaging, Plasmon Waveguide Resonance (PWR) and others, have been increasingly used to determine the affinity and kinetics of a wide variety of real time

molecular interactions such as protein-protein, lipid-protein and ligand-protein, without the need for a molecular tag or label [6]. The electrochemical sealing properties of the mono- and bilayer can be investigated using electrochemical impedance spectroscopy (EIS) [7]. The QCM-D technique has proven very valuable to screen the overall properties of the lipid deposition, thanks to the dissipation parameter that allows distinguishing between intact, adsorbed vesicles (high dissipation) and bilayer patches (low dissipation) [1]. Apart from these, neutron reflectivity (NR) is an ideal tool to study buried interfaces, and thus it is possible to determine the structure of tBLMs formed by the different anchor lipids [8].

Higher-resolution images of small defects in the 10 to 500 nm range can be obtained by atomic force microscopy (AFM) or near-field fluorescence microscopy (NSOM) [9].

1.1 .Purpose of Thesis

In this study, the liposomes with different compounds and different compositions were prepared in order to investigate the effect of membrane composition on tBLMs formation. For this, unilamellar liposomes with different phospholipid content (phosphatidylcholine (PC), phosphatidylserine (PS) and phosphatidylethanolamine (PE)) was used. Surface plasmon resonance (SPR) that is commonly used for real-time, label-free evaluation of binding and interactions of biological molecules in liquid environment was used to investigate the liposomal binding. Interpretation of SPR data was also complemented with quartz crystal microbalance with dissipation (QCM-D) analysis to determine mass and viscoelastic properties of thin lipid films.

2. BACKGROUND INFORMATION

2.1 Lipids

Lipids play a variety of roles in biological systems. They are molecules that are insoluble in water and soluble in organic solvents. The diversity of lipids can be very high due to the complexity of the hydrophobic acyl chains (i.e. carbon number and degree of unsaturation) and the nature of the hydrophilic polar head group [10].

All lipids are hydrophobic or amphipathic in nature [11]. It is the shape and amphipathic nature of the lipid molecules that cause them to form bilayers spontaneously in aqueous environments. Lipid molecules spontaneously aggregate to bury their hydrophobic tails in the interior and expose their hydrophilic heads to water. Depending on their shape, they can do this in either of two ways: they can form spherical micelles, with the tails inward, or they can form bimolecular sheets, or bilayers, with the hydrophobic tails sandwiched between the hydrophilic head groups (Figure 2.1) [12].

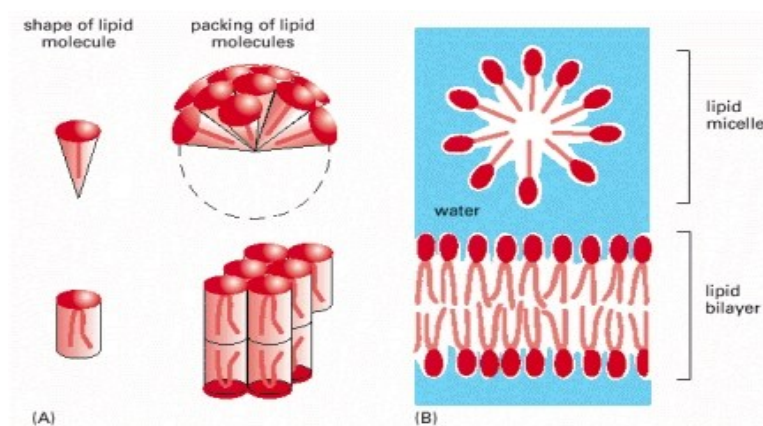


Figure 2.1 : Packing arrangements of lipid molecules in an aqueous environment (A) Wedge-shaped lipid molecules (*above*) form micelles, whereas cylinder-shaped phospholipid molecules (*below*) form bilayers. (B) A lipid micelle and a lipid bilayer seen in cross section. Lipid molecules spontaneously form one or other of these structures in water, depending on their shape.

Lipids can be divided into non-polar lipids (e.g. triglycerides and cholesterol) and polar lipids (e.g. phospholipids, glycolipids, and sphingolipids) based on the number

of primary products formed after hydrolysis (Figure 2.2) [10]. Although the role of lipids in the cellular area is still not fully understood, they are generally believed to be used for energy storage, serve as structural components of cell membranes, and constitute important signaling molecules [11].

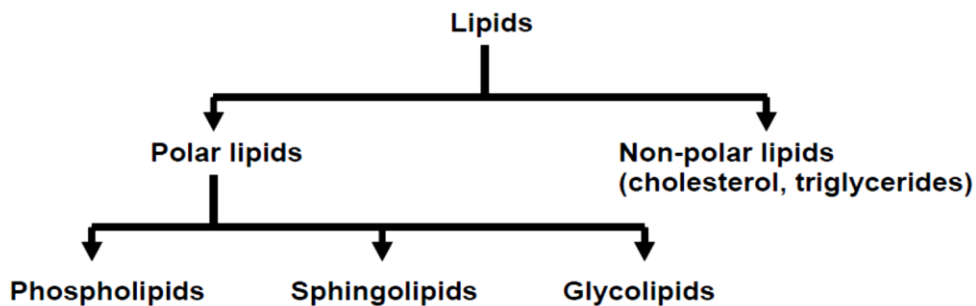


Figure 2.2: Classification of Lipids.

It was only around 1970 that researchers first recognized that individual lipid molecules are able to diffuse freely within lipid bilayers. The initial demonstration came from studies of synthetic lipid bilayers. Two types of preparations have been very useful in such studies: (1) bilayers made in the form of spherical vesicles, called liposomes, which can vary in size from about 25 nm to 1 μm in diameter depending on how they are produced (Figure 2.3) (Liposomes are commonly used as model membranes in experimental studies.) and (2) planar bilayers, called black membranes, formed across a hole in a partition between two aqueous compartments (Figure 2.4). This planar bilayer appears black when it forms across a small hole in a partition separating two aqueous compartments. Black membranes are used to measure the permeability properties of synthetic membranes [12].

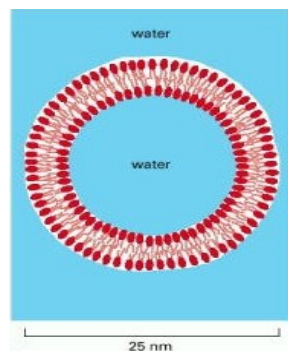


Figure 2.3: A drawing of a small spherical liposome seen in cross section.

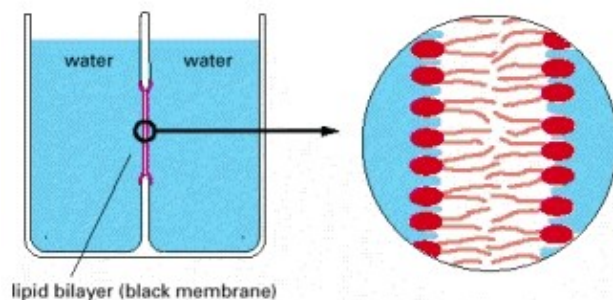


Figure 2.4: A cross-sectional view of a black membrane, a synthetic lipid bilayer.

2.2 Phospholipids

Phospholipids are composed of a glycerol backbone with fatty acids esterified at adjacent carbon positions; while a polar head group is attached to a phosphate ester group at the remaining carbon [13].

The amphiphilic nature of membrane phospholipids has been well known to form the bilayer that is necessary for proteins to function and interact. A second function of phospholipids is to serve as the source of arachidonic acid, which is required for the formation of lipid mediators such as leukotrienes and prostaglandins. They are also the precursors for platelet-activating factor and signaling molecules such as inositol triphosphate and diacylglycerol [13]. Furthermore, synthetic phospholipids have been used as drug carriers in the pharmaceutical industry [14].

Phospholipids nomenclature is based on the polar head group. The structure of selected phospholipids for this study (phosphatidylcholine (PC), phosphatidylethanolamine (PE) and Phosphatidylserine (PS)) are shown in Figure 2.5.

Mammalian cell membranes contain >1,000 different phospholipids. The amounts of the various phospholipids in a membrane define the fluidity of the membrane and the functions of the embedded proteins [15]. Four major phospholipids predominate in the plasma membrane of many mammalian cells: phosphatidylcholine (PC), phosphatidylethanolamine (PE), phosphatidylserine (PS), and sphingomyelin. Note that only phosphatidylserine carries a net negative charge, the other three are electrically neutral at physiological pH, carrying one positive and one negative charge. Together these four phospholipids constitute more than half the mass

of lipid in most membranes. Other phospholipids, such as the inositol phospholipids, are present in smaller quantities but are functionally very important. The inositol phospholipids, for example, have a crucial role in cell signaling [12].

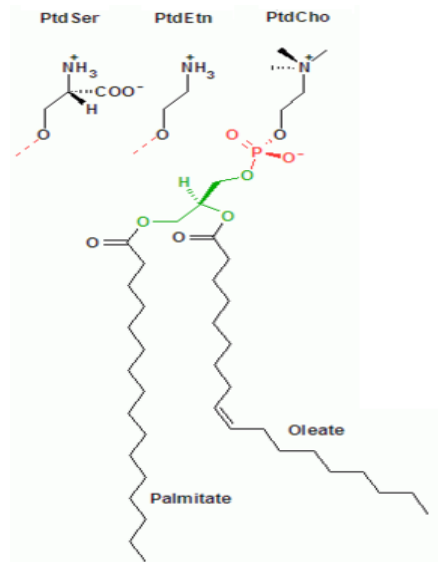


Figure 2.5: The chemical structures of phosphatidylserine (PtdSer), phosphatidylethanolamine (PtdEtn) and phosphatidylcholine (PtdCho).

Phosphatidylcholine is the most abundant phospholipid in mammalian cell membranes, constituting 40–50% of total phospholipids [15]. PC not only plays a critical role in the manufacture of primary cell membrane components, but it is also essential in the synthesis of acetylcholine. Clinical studies have shown that PC can increase serum acetylcholine levels, which play a crucial role in many brain processes [10].

The second most abundant mammalian membrane phospholipid is phosphatidylethanolamine (PE), which constitutes 20–50% of total phospholipids. In the brain, ~45% of total phospholipids are PE, whereas in the liver, only ~20% of total phospholipids are PE [15]. PE also performs numerous biological roles beyond serving a structural role in membranes. For example, PE metabolism in the heart appears to be important, because the asymmetrical transbilayer distribution of PE in sarcolemmal membranes is altered during ischemia, leading to sarcolemmal disruption [16]. In addition, PE is required for contractile ring disassembly at the cleavage furrow of mammalian cells during cytokinesis [17]. The different organelles within mammalian cells also have distinct phospholipid compositions. In

mitochondria, particularly in the inner membrane, the PE content is significantly higher than in other organelles [15].

Phosphatidylserine (PS) is a quantitatively minor membrane phospholipid that makes up 2–10% of total phospholipids. The brain is enriched in the two aminophospholipids PE and PS compared with other tissues. In the brain, and particularly in the retina, the acyl chains of PS are highly enriched in docosahexaenoic acid (22:6n-3). In human gray matter, 22:6n-3 accounts for >36% of the fatty acyl species of PS. Because 22:6n-3 appears to be essential for the normal development and functioning of the nervous system, it is likely that PS plays an important role in the nervous system and in vision [15]. In resting cells plasmalemmal PS is found exclusively on the inner (cytoplasmic-facing) monolayer, due to the action of ATP-dependent aminophospholipid flippases [18]. Moreover, animals exploit the phospholipid asymmetry of their plasma membranes to distinguish between live and dead cells. When animal cells undergo programmed cell death, or apoptosis, phosphatidylserine, which is normally confined to the cytosolic monolayer of the plasma membrane lipid bilayer, rapidly translocates to the extracellular monolayer. The phosphatidylserine exposed on the cell surface serves as a signal to induce neighboring cells, such as macrophages, to phagocytose the dead cell and digest it [12].

2.3 Biomimetic Model Membrane Systems

Biological membranes play a fundamental role in cell life. The cell membrane hosts a wide variety of signaling molecules, and often selectively compartmentalizes these molecules into microdomains so specific functions are enabled. Given the complexity in compositions and organization, biomembranes are difficult to be studied in details in live cells [19]. Therefore, many different model systems have been created that retain the essential lipid bilayer structure, and simplify the system so that the roles of individual components can be assessed and that their organization and dynamics can be visualized [20]. Moreover, increasing the stability of biomimetic systems has been of critical importance with their applicability to such fields as biosensors, drug delivery, biocatalysis, and cellular recognition, which rely on high stability to remain functional in an electronically interfaced environment [21].

Currently, models of biological membranes include liposomes and giant vesicles in solution, lipid monolayers at the air-water-interface, black lipid films, membrane patches at pipettes, or solid-supported membranes (Figure 2.6) [3].

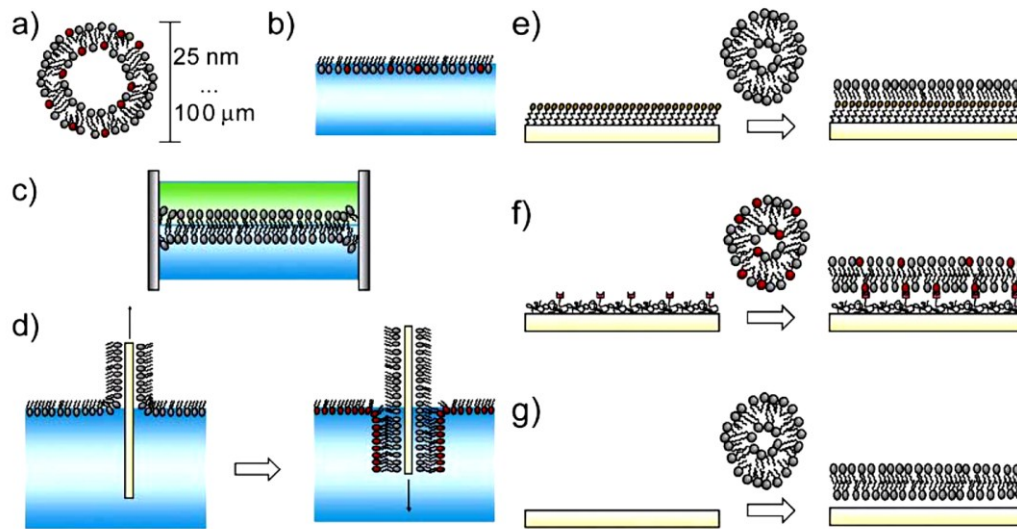


Figure 2.6: Models of biological membranes. (a) liposomes (25 nm to 100 μm in diameter); (b) lipid monolayers at the air-water interface; (c) black lipid membranes suspended over an aperture between two aqueous phases; (d) Langmuir-Blodgett method allowing the transfer of lipid mono- and multi-layers from the air-water interface to a solid support; (e) self-assembled monolayer on glass/gold/silica surface; (f) polymer cushioned bilayer; (g) spontaneous spreading of liposomes on surface.

In the classical liposomal system the lipid bilayer encloses an inner cavity. Therefore, experimental difficulties arise when there is a need to control contents or solute concentrations of the inner compartment. The same holds for the application of a transmembrane potential that is limited to the generation of a diffusion potential by the usage of ion-specific ionophores [22]. These problems do not arise when using black lipid membranes (BLMs) that provide equal access to both sides of a membrane. However, BLMs lack mechanical and long-term stability. For both of these systems it is impossible to apply surface-sensitive techniques such as AFM, SPR, QCM, or ATR-FTIR, and will probably never evolve to a routinely used and/or large-scale technology for biosensing or lab-on-a-chip applications [4].

To overcome these problems, the two most stable and commonly used cell membrane biomimetic systems are supported bilayer lipid membranes (sBLMs) and tethered bilayer lipid membranes (tBLMs).

Supported bilayer lipid membranes are commonly formed on monolayer templates, hydrophilic substrates, or polymer cushions and are known to maintain the physiological and chemical properties of natural bilayers. However, the success of sBLMs as a biomimetic system has been limited by their lack of an aqueous reservoir between substrate and membrane [21]. This may give rise to certain limitations to study membrane proteins due to immobilization-induced conformational changes of proteins and substrate-induced constraints in lipid mobility and protein conformations [19]. Further, sBLMs are practically limited due to their poor stability upon exposure to air [23].

Several classes of proteins are transporters and require sufficient aqueous media on both sides of the membrane to function; tBLMs do provide these conditions. Tethered bilayer lipid membranes are often formed using lipids with thiol, disulfide, and silane modified headgroups, depending on the substrate, and are separated from the substrate by a hydrophilic spacer [24] [25] [26]. Self-assembled monolayers (SAM) of such molecules form an amphiphilic supramolecular array of a lipid film with a hydrophilic submembrane space, mimicking the cytosol [21] [26].

Recently, tBLMs have been taken advantage of small ion conducting peptides, such as gramicidin and valinomycin, as well as macromolecular proteins such as cytochrome c oxidase. Moreover, the growing interest in biosensors using ion channels as switches has led to tBLMs becoming one of the choice model systems for this application [21]. Due to the covalent attachment of the linker to the surface, the tethered molecules endow the lipid film with a robustness much greater than that of the bilayer lipid membrane (BLM). The planar arrangement, particularly on a metal substrate, allows for the application of a variety of surface-sensitive analytical techniques. The metal surface allows for the investigation of the lipid bilayer under a defined electric field. Hence, tBLMs are useful in basic research, particularly as far as membrane proteins are concerned, but also for biosensor applications [26].

Among these, PEG-based coatings are probably the most successful example and have therefore become a standard concept in controlling the interface between (bio)materials and biology in general, from drug delivery applications to biosensing [27]. PEG is a hydrophilic polymer that swells significantly in aqueous environments [28]. Surface-grafted PEG substantially reduces the adsorption of proteins and cells. Additionally, PEG does not display any antigenic activity. These properties have

made platforms such as PEG-grafted liposomes popular for drug delivery and other therapeutic treatments. PEG provides a barrier around the liposomes, protecting them from rupture and thereby increasing their circulation time. The hydrophilic character of PEG along with its weak interactions with proteins and lipids has made PEG attractive for use as a cushion for supported lipid bilayers. Such supported lipid bilayers have been proposed for use in applications such as biosensors or as models to study the structure and function of biomembranes [29].

2.4 Surface Plasmon Resonance (SPR)

The study and characterization of molecular interactions is essential to explore biomolecular structure-function relationships, and it aids our understanding of biological systems in life sciences. Surface plasmon resonance (SPR) biosensors present a powerful optical label-free biosensor technology that has been widely applied to the investigation of biomolecular interactions and the detection of chemical and biological analytes [30]. Compared to conventional techniques, SPR biosensors speed up such investigations as drug development, immunoreagent quality control, cell adhesion studies and polymer-biomolecule interactions (Figure 2.7).

In addition, multichannel SPR biosensors make it possible to observe large numbers of biomolecular interactions and identify and simultaneously quantify multiple biomarkers [31].

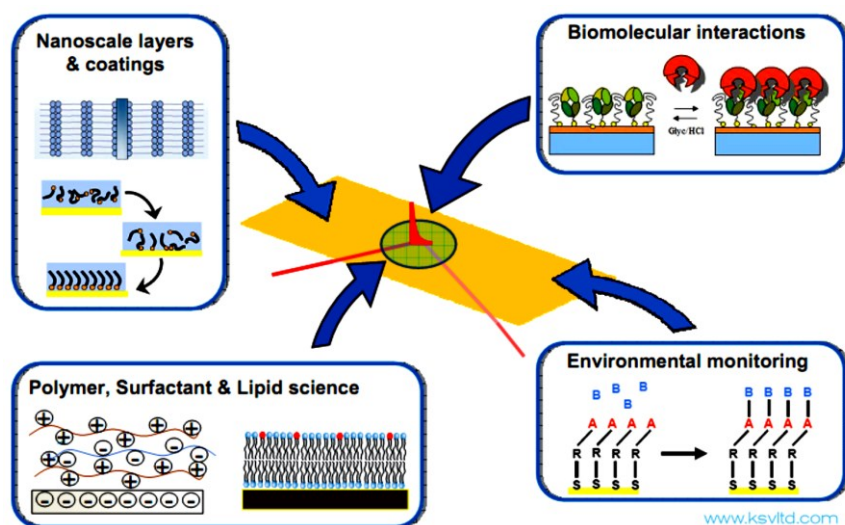


Figure 2.7: Main Application areas of SPR Technology.

2.4.1 Principle of SPR

In principle, SPR sensors are thin-film refractometers that measure changes in the refractive index occurring at the surface of a metal film supporting a surface plasmon [32] [33] [34].

SPR refers to the optical excitation of surface plasmons or charge-density waves at the interface between a conductor and a dielectric. The conductor is a metal (gold or silver) that has a high free-electron density to support the charge-density waves. The dielectric can be a gas, a liquid, or a solid. Surface plasmons are collective oscillations of free electrons in a metallic film [35]. Under appropriate conditions, the plasmons can be made to resonate with light, which results in the absorption of light [35] [34].

The excitation of surface plasmon is accompanied by the transfer of optical energy into surface plasmon and its dissipation in the metal layer, which results in a narrow dip in the spectrum of reflected light. Surface plasmon waves (SPWs) are extremely sensitive to small changes in the refractive index near the sensor surface and the changes in the refractive index are proportional to the sample mass, so the adsorption of molecules on the metal film or conformational change in the adsorbed molecules can be detected accurately (Figure 2.8) [33].

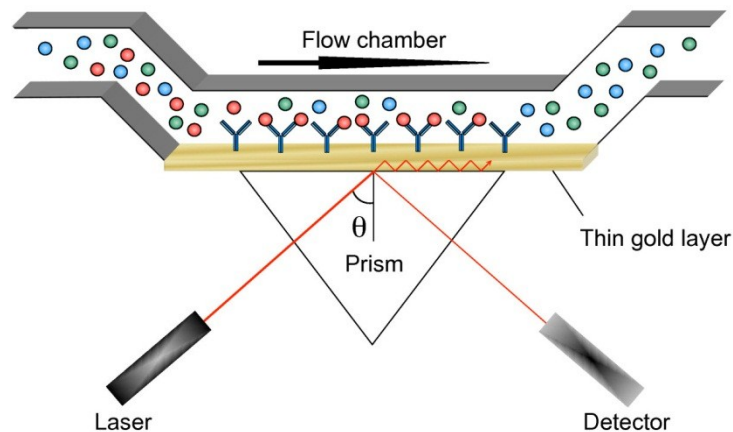


Figure 2.8: Schematic illustration of SPR Phenomena.

In order to detect an interaction, a molecule (the ligand) is immobilised onto the sensor surface and, its binding partner (the analyte) is injected in aqueous solution (sample buffer) through the flow cell, also under continuous flow. As the analyte binds to the ligand the accumulation of analytes on the surface results in an increase in the refractive index. This change in refractive index is measured in real time, and

plotted as response or resonance units (RUs) versus time (a sensorgram). The adsorption–desorption process can be followed in real time and the amount of adsorbed species can be determined (Figure 2.9) [32].

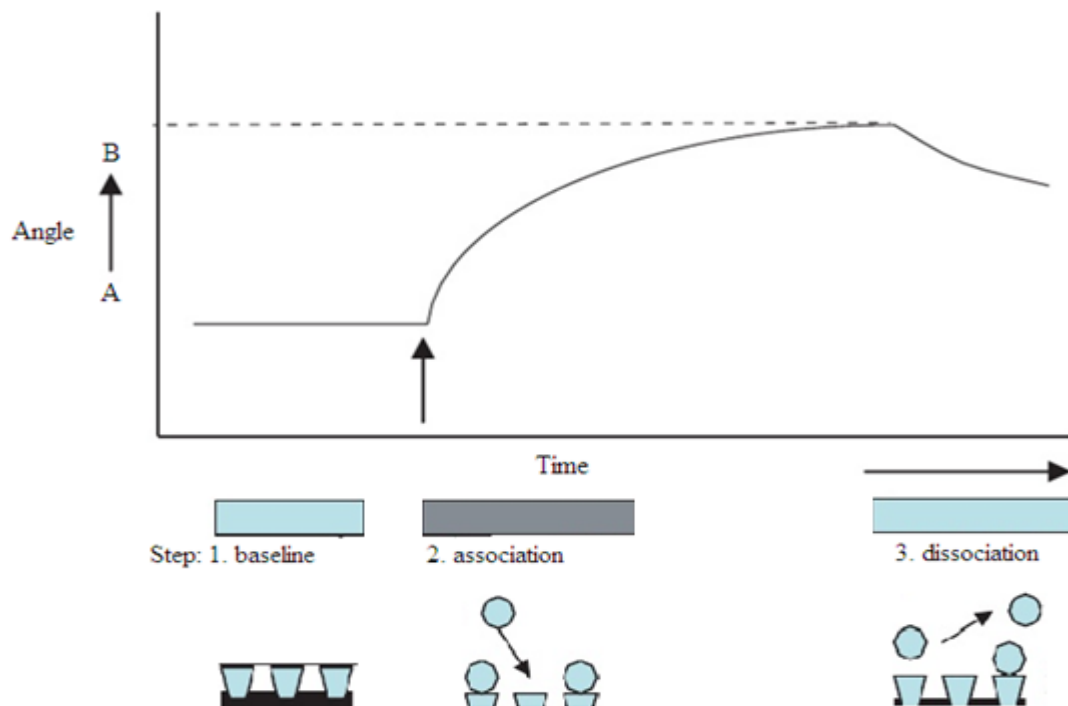


Figure 2.9: A sensorgram: the angle at which the dip is observed vs. time. First, no change occurs at the sensor and a baseline is measured with the dip at SPR angle (A). After injection of the sample (arrow) biomolecules will adsorb on the surface resulting in a change in refractive index and a shift of the SPR angle to position B.

Importantly, a response (background response) will also be generated if there is a difference in the refractive indices of the running and sample buffers. This background response must be subtracted from the sensorgram to obtain the actual binding response. The background response is recorded by injecting the analyte through a control or reference flow cell, which has no ligand or an irrelevant ligand immobilized to the sensor surface [32].

2.5 Quartz Crystal Microbalance with Dissipation (QCM-D)

The QCM is basically a mass sensing device with the ability to measure very small mass changes on a quartz crystal resonator in real-time. It has proved to be a valuable instrument for the study of membrane-bound proteins, membrane mediated cellular

processes, protein-lipid interactions, cell-cell interactions, antibody-antigen interactions, biological signal transduction, and drug delivery detection [36].

Studying vesicle interactions with solid surfaces using the QCM-D technique is initiated by Kasemo and coworkers (1998) and vesicle fusion became an established tool to form SLBs due to the ability of QCM-D to characterize the entire process in real-time, including the quality as well as the kinetic analysis of the formed bilayer [37].

2.5.1 Basic Principle of QCM-D

A QCM is an ultra-sensitive mass sensor utilizing the piezoelectric properties of quartz crystals. The QCM can detect adsorbed and desorbed masses in the nanogram range in real time. It consists of a piezoelectric quartz crystal sandwiched between a pair of electrodes. When the electrodes are connected to an oscillator and an AC voltage is applied over the electrodes the quartz crystal starts to oscillate at its resonance frequency due to the piezoelectric effect. Any mass loss or addition on quartz crystal surface will change the frequency [38]. Sauerbrey found that the resonance frequency decreases linearly if additional mass is attached to the sensor (2.1) [39]. Sauerbrey equation, written to include harmonic resonances, is

$$\Delta m = -C(\Delta f_n/n) \quad (2.1)$$

where Δm is the adsorbed mass on the surface, C is the mass sensitivity constant ($17.7 \text{ ng} \cdot \text{cm}^{-2} \cdot \text{Hz}^{-1}$ at $f = 5 \text{ MHz}$), and Δf_n is the change in the resonance frequency at the n^{th} harmonic. The harmonic order n has values (1,3,5,...). C is a constant independent of the harmonic order n . If the Sauerbrey relation is satisfied, then the normalization of the observed frequency change at the n^{th} harmonic by n should yield a constant value. If an ideal rigid layer is assumed, eq 1 has been demonstrated to provide an accurate modeling fit [40]. However, this is only true if the attached mass is rigid and small compared to the sensor mass [39].

Two reasons explain the deviations from the Sauerbrey relation. One reason is that the adlayer may be viscoelastic, as in the case of adsorbed vesicles, which gives rise to a compound resonator for which Δf is not directly proportional to Δm . In this case, the frequency change becomes sensitive to the mechanical properties of the film, including the shear modulus and viscosity. The other reason is that the molar mass

(or dry mass) by itself is insufficient to describe the film mass. The mass of water, associated with the film, must also be included. For vesicle adsorption on a gold surface that results in a soft layer, the water may appear to contribute to the mass increase due to direct hydration, coupling between vesicles, or entrapment on a roughened surface [40].

The resonance frequency of acoustic resonators depends on temperature, pressure and bending stress. Temperature-frequency coupling is minimized by employing special crystal cuts. A widely used temperature-compensated cut of quartz is the AT-cut (Figure 2.10) [36] [38]. Careful control of temperature and stress is essential in the operation of the QCM. AT-cut crystals are singularly rotated Y-axis cuts in which the top and bottom half of the crystal move in opposite directions (thickness shear vibration) during oscillation [38].

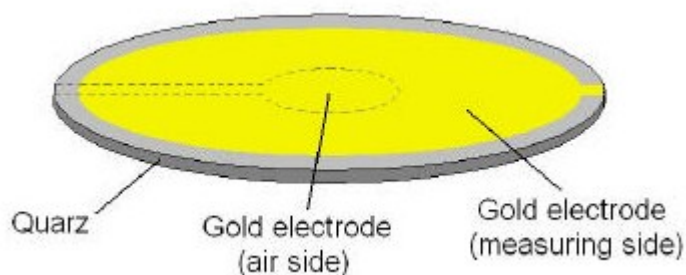


Figure 2.10: Schematic illustration of AT-cut quartz crystal.

2.5.2 The dissipation

The damping or dissipation (D) includes information on the film's viscoelasticity. D is defined as the ratio of energy lost (dissipated) during one oscillation cycle to the total energy stored in the oscillator **(2.2)** [41]

$$D = E_{lost} / 2\pi \times E_{stored} \quad (2.2)$$

As the size and structural flexibility of the adsorbed molecules increases, the importance of measuring the dissipation also increases. Combined f and D measurements along with the appropriate theory can provide a way to test for a linear relationship of the simple Sauerbrey model. Furthermore, by plotting Δf versus ΔD , information about conformation of the adsorbed materials may be extracted and a so-called reaction fingerprint described (i.e., how the mass adsorbed changes, approximated by Δf , with the viscoelastic characteristics, approximated by ΔD).

Also, by monitoring both Δf and ΔD it is possible to quantify and separate the viscoelastic variables relating to the shear viscosity and storage modulus of the adsorbed materials (Figure 2.11) [42].

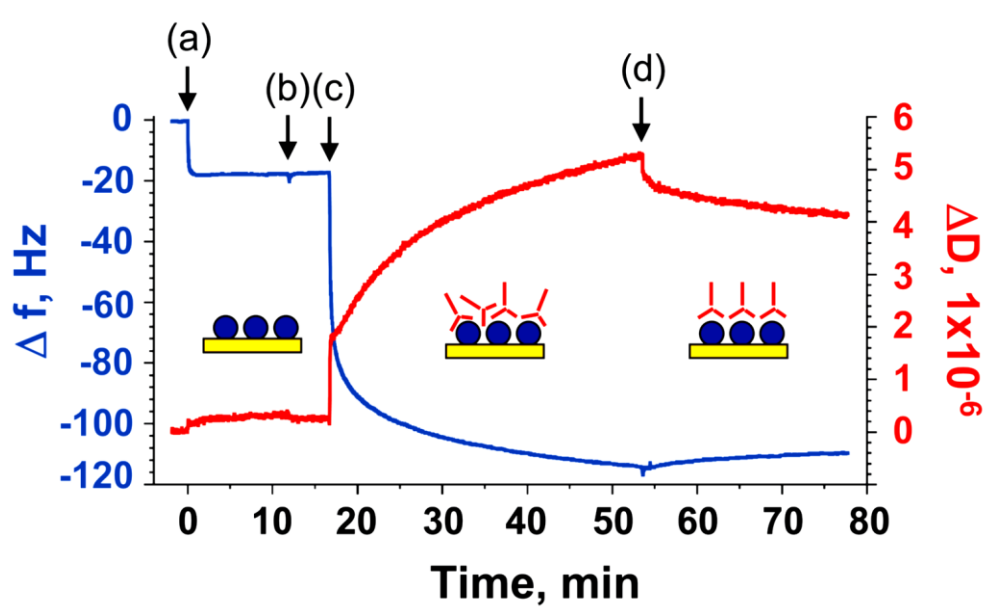


Figure 2.11: Example of raw data from a QCM-D experiment. This particular example demonstrates the adsorption of rigid (a) and soft molecules (c). Steps b and d correspond to buffer rinses. Frequency changes (Δf) are shown in blue on the left axis and dissipation changes (ΔD) are shown in red on the right axis [43].

3. MATERIALS AND METHODS

3.1 Material

The phospholipids: phosphatidylethanolamine (PE) and phosphatidylserine (PS) were purchased from Avanti Polar Lipids (Alabaster, AL, USA), phosphatidylcholine (PC) from Sigma-Aldrich (St. Louis, MO, USA). Dimethyl sulfoxide (DMSO) and chloroform were purchased from Merck (Whitehouse Station, NJ, USA). 1,2-distearoyl-sn-glycero-3-phosphoethanolamine-N-[amino (polyethylene glycol)-2000 (DSPE-PEG) was from Avanti Polar Lipids (Alabaster, AL, USA). 3,3'-dithiodipropionic acid di(N-hydroxysuccinimide) (DTSP) was purchased from Sigma-Aldrich (St. Louis, MO, USA).

3.2 Equipments

3.2.1 Surface plasmon resonance (SPR)

SPR measurements were performed with Reichert SR7000 Single Channel Surface Plasmon Resonance Spectrometer (Figure 3.1). The formation of tBLMs was observed on an SPR sensor chip (BK7 glass thickness: 0.95 mm; chromium thickness: 1nm; gold thickness: 50nm). A peristaltic pump of which flow rate was $350 \mu\text{L min}^{-1}$ and tubings (Tygon, SC0060) were used for piping solutions onto gold slides. All measurements were performed at 25 °C. Mass changes at the interface between the gold layer and the aqueous compartment cause changes in the local refractive index near the gold layer. The changes of refractive index were monitored by computer in real time.



Figure 3.1: SR7000 Single Channel Surface Plasmon Resonance Spectrometer.

3.2.1.1 Preparation of SPR set-up

Prior to each experiment, all parts of the set-up was cleaned. Measurement chamber was cleaned by 70% solution of ethanol and dried. Tubings were cleaned by passing through 1% solution of SDS and then rinsed with purified water. After these steps, a drop of immersion oil was placed between the prisma and the slide surface. Finally, the whole measurement cell was assembled.

Sonication was used to remove dissolved gases from the solutions such as dH₂O and PBS.

3.2.2 Quartz crystal microbalance with dissipation monitoring (QCM-D)

QCM-D measurements were performed with QCM-Z500 (KSV Instruments) in a flow-through cell (Figure 3.2). A peristaltic pump and tubings (Tygon, R3607, ID: 1.09 mm, wall thickness: 0.86 mm) were used to transport analyte solutions to the quartz crystal surface. The experiments were performed under a volume flow rate of 112 $\mu\text{L min}^{-1}$. All measurements were performed at 25 °C. The changes of frequency were monitored by computer in real time and data from one fundamental and four overtone frequencies (15, 25, 35, 45 MHz) were collected. These frequencies correlate with the third, fifth, seventh, ninth and eleventh harmonics ($n=3, 5, 7, 9$). The frequency shifts were normalized to the fundamental frequency by division with the overtone number n .

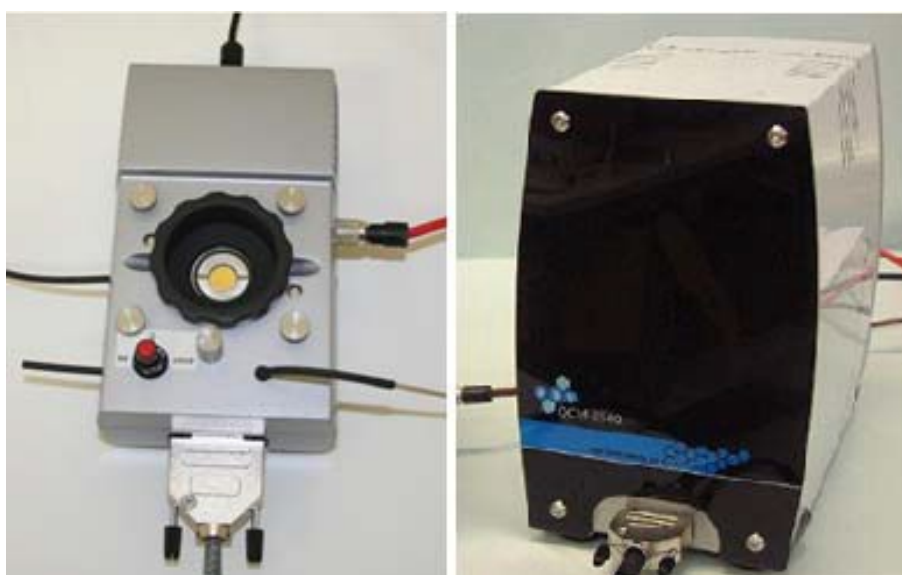


Figure 3.2: The fully assembled QCM and the electronic unit.

3.2.2.1 Preparation of QCM-D set-up

Before each experiment, the fluid cell, tubings and o-ring were thoroughly cleaned by 70% solution of ethanol and after that, they were repeatedly rinsed with purified water. Then, the fluid cell and o-ring were dried under nitrogen.

After cleaning all the parts of QCM-D set-up, first o-ring and then quartz crystals with gold coating were inserted into the measurement chamber by the help of a tweezer (Figure 3.3). Finally, the whole system was assembled firmly to allow crystals to contact with samples directly and prevent leaking of solutions.



Figure 3.3: The insertion of o-ring and quartz crystals.

3.3 Construction of Tethered Bilayer Lipid Membranes (tBLMs)

Construction of tBLMs has three major steps (Figure 3.6). First of all, DTSP (3,3'-dithiodipropionic acid di(N-hydroxysuccinimide)) (Figure 3.4) layer was formed on the gold surface out of the SPR or QCM system. Second, DSPE-PEG(1,2-distearoyl-sn-glycero-3-phosphoethanolamine-N-[amino (polyethylene glycol)-2000] (ammonium salt)) (Figure 3.5) layer was constructed as a second layer and monitored by SPR or QCM-D. Finally, liposomes were spreaded on the gold surface to form tBLMs and monitored by SPR or QCM-D.

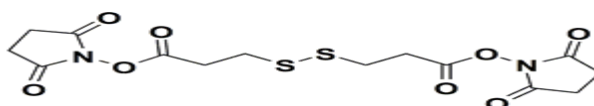


Figure 3.4: Structural formula of DTSP.

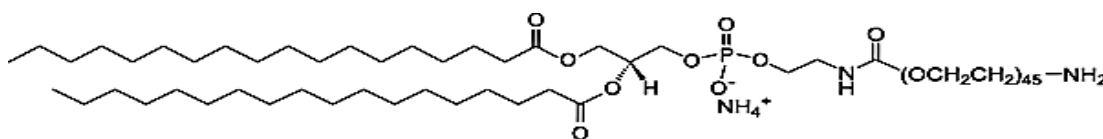


Figure 3.5: Structural formula of DSPE-PEG.

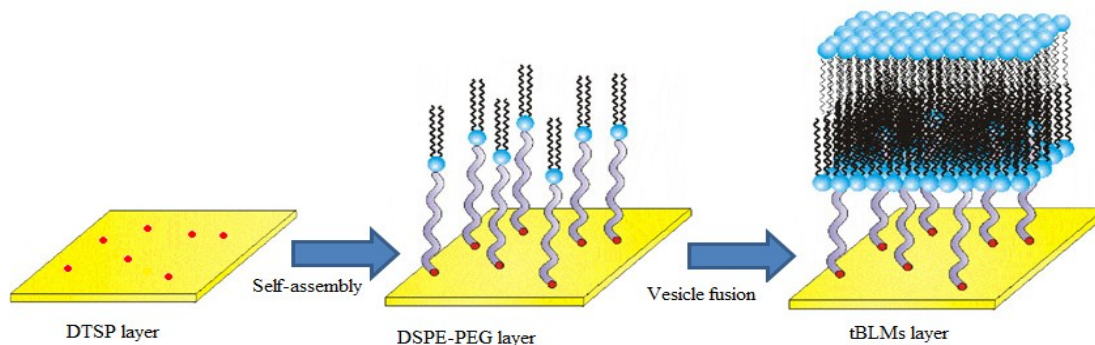


Figure 3.6: This figure illustrates construction of tBLMs layer on the gold surface [44].

3.3.1 Functionalization of the gold films

DTSP is a homobifunctional and cleavable crosslinker. DTSP has amine-reactive N-hydroxysuccinimide (NHS) esters at both ends of a cleavable, 8-atom (12.0 angstrom) spacer arm. DTSP crosslinking reagent contains a reducible disulfide (thiol) bond in the spacer arm that binds covalently to gold surface and generates self-assembled monolayer (SAM).

DTSP must be dissolved in an organic solvent. Thus, first of all, this molecule was dissolved in 1 mM DMSO. Both gold surfaces for SPR slides and quartz crystals, to be prepared for SPR and QCM measurements, respectively, were immersed in a solution of dithiobis (succinimidyl propionate) (DTSP; 1mM in DMSO) for overnight. Surface activation performed in a closed box that was covered with aluminum foil to prevent activator from the negative effects of light. After this procedure, the SPR slides and quartz crystals were rinsed with acetone and dried under a stream of nitrogen.

3.3.2 Construction of DPSE-PEG as a second layer

Initially, degassed dH₂O was sent to the system to obtain a constant resonance frequency. Subsequently, DSPE-PEG(2000) (1,2-distearoyl-sn-glycero-3-phosphoethanolamine-N-[amino (polyethylene glycol)-2000]; 0.03 mg/mL in dH₂O) was pumped to the system and waited for saturation. DSPE-PEG molecule, which was used as the second layer, has a role as the tethering molecule for the tBLMs. In order to wash out unbound DSPE-PEG molecules, dH₂O was passed through the system.

3.3.3 Preparation of liposomes and construction of tBLMs as a third layer

Phosphatidylcholine (PC), phosphatidylethanolamine (PE) and phosphatidylserine (PS) were dissolved separately in chloroform at +4°C as a stock solution (1 mg/mL), aliquoted and stored at -20°C. To prepare thin lipid film layer, lipid solution which was obtained by mixing different lipid compositions (Table 3.1) was poured into a round-bottom flask. Chloroform was evaporated using a dry nitrogen stream in a fume hood and the lipid film layer was left at +4 °C overnight.

Table 3.1: Different lipid compositions.

Lipid composition	Molar ratio
PC	1
PE	1
PS	1
PC:PE	1:9
	1:3
	0,5:0,5
	3:1
	9:1
PC:PS	1:9
	1:3
	0,5:0,5
	3:1
	9:1

The obtained thin lipid film layer was suspended in 5 ml 0.1 M PBS (pH 7.4) and then vortexed vigorously. Final lipid concentration was 0.02 mg/ml. Liposomes were generated by the help of an extruder (Avanti Mini-Extruder) (Figure 3.7). The resulting liposomes were extruded 15 times through a 100 nm polycarbonate membrane and stored at +4 °C. At the end of this stage, the syringes of extruder were washed by isopropanol and teflon parts were cleaned by ethanol and stayed in ethanol solution.

To construct tBLMs as a third layer of the system, first PBS was sent to DSPE-PEG bound surface to obtain a constant baseline and then liposome solution was pumped through the system till saturation was observed. Finally, the system was rinsed with PBS in order to withdraw unbound liposomes and lipids from the system.



Figure 3.7: The whole extruder system.

4. RESULTS & DISCUSSION

4.1 Effect of membrane composition

A number of processes can occur when a liposome encounters a surface. Adsorption is associated with membrane deformation (likely flattening). At sufficiently large deformations, a liposome may rupture and transform into a bilayer disk. Alternatively, neighboring vesicles may interact, or fuse, before rupturing into membrane patches. Bilayer disks or membrane patches may coalesce and/or induce the rupture of adsorbed vesicles. The relative contribution of these interactions is affected from the nature of the support (its surface charge, structure, and roughness) and the lipid vesicles (their composition, charge, size, and physical state), as well as the aqueous environment (the pH and ionic strength) [3].

In this study, the construction of the DSPE-PEG-tethered lipid bilayers on DTSP modified gold surface was monitored by surface plasmon resonance spectroscopy (SPR) and quartz crystal microbalance with dissipation (QCM-D). The liposomes with different compounds and different compositions were prepared in order to investigate the effect of membrane composition on tBLMs formation. tBLMs were formed according to the procedure optimized in our group [45]. Either SPR gold covered slides or QCM gold covered crystals were modified by dithiobis (succinimidyl propionate) (DTSP; 1mM in DMSO). DTSP crosslinking reagent contains a reducible disulfide (thiol) bond in the spacer arm that binds covalently to gold surface and generates self-assembled monolayer (SAM). Then, DSPE-PEG(2000) (0.03 mg/ml in dH₂O) was attached on it to serve as tethers for tBLMs. Finally, liposomes of different lipid composition were generated by the help of an extruder using 100 nm membranes and were spread onto the modified surface. A gold substrate was used as a solid support allowing for the lipid bilayers to be characterized by SPR or QCM-D.

4.1.1 Formation of DSPE-PEG monolayer

DSPE-PEG was employed as a spacer molecule to tether the proximal lipid layer to the DTSP modified gold surface thus providing good stability and preserving the native liquid-crystalline state of the bilayer on the support. PEG is a hydrophilic polymer that swells significantly in aqueous environments [28]. The swelling would also cause an increase in the monolayer thickness [26] and this increase could be monitored via surface plasmon resonance (SPR) as increase in optical thickness as shown in Figure 4.1. Additionally, frequency change was observed by using quartz crystal microbalance (QCM).

Optimum DSPE-PEG concentration providing the best conditions for tBLMs formation by PC liposomes has been shown to be 0.03 mg/ml [45]. Because of that, 0,03 mg/ml of DSPE-PEG solution was used to investigate tBLMs formation of different lipid compositions in this study.

The kinetics of monolayer formation of DSPE-PEG was very fast and saturated after 15 min. for SPR and after about 1 h. for QCM. The difference in time scale could be explained by difference in injection mode and difference in cell chamber of SPR and QCM-D. There was a change approximately 1250 μ RIU in refractive index and -34 Hz in frequency. DSPE-PEG monolayer was not affected after rinsing by dH₂O (Figure 4.1).

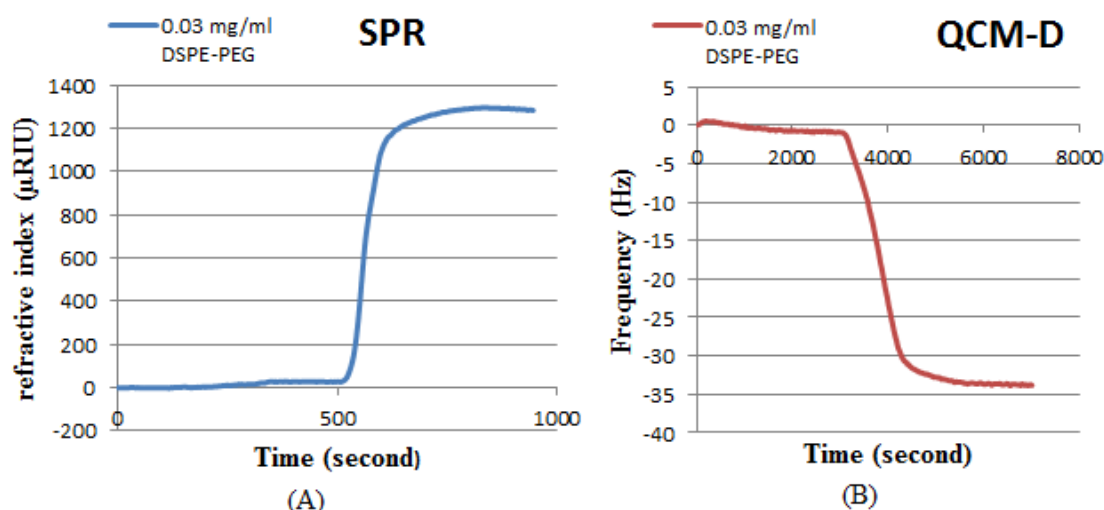


Figure 4.1: Change in SPR refractive index (A) and QCM-D frequency (B) versus time demonstrating the interaction of DSPE-PEG with DTSP covered gold surface to form the second layer.

4.1.2 The effects of percentage of PE on PC/PE liposomes

The adsorption behavior of zwitterionic PC and PC/PE liposomes onto DSPE-PEG modified gold surface was investigated by SPR and QCM-D. For molecules adsorbing to the sensor surface, thereby changing the local refractive index, the shift of the resonance angle, is proportional to the surface concentration of the molecules and is recorded in a sensorgram. The response remains constant if the interaction reaches equilibrium. Change in SPR results were shown in μ RIU (micro refractive index unit) range.

The binding studies of zwitterionic PC/PE liposomes prepared in different compositions shown in Table 3.1 and lipid bilayer formation was monitored in real-time on DTSP covered gold slides by SPR. The lipid concentration was 0.02 mg/ml. At least 2-3 experiments were performed for each data point.

It could be seen from Figure 4.2 that when the amount of PE increased on liposomes, change in refractive index increased remarkably compared with PC liposomes (except PE and 90PC/10PE liposomes). Change in refractive index indicated an increase in the thickness due to binding of vesicles.

After the washing procedure, RI, reached a plateau within 50 minutes except for 10PC/90PE and PE liposomes. RI values for PC/PE (75/25, 50/50, 25/75 and 10/90) liposomes reached approximately the same level ($RIU_{max} = \sim 3800 \mu$ RIU) upon incubation. However, 10PC/90PE liposomes were highly affected from washing step ($RIU_{fin} = 1680 \mu$ RIU) and experiment lasted approximately 3 hours for the system to reach a plateau.

Similar behavior was observed for PE liposomes: The signal was stabilized at 907 μ RIU after rinsing and it lasted 2.5 hours. These values are significantly higher, compared to tBLMs formation in PC liposomes studies which were optimized by our group [45].

In this study, PC liposomes caused a maximum RI change of 2380 μ RIU and after rinsing RIU_{fin} was found to be 1470 μ RIU. Also, change in refractive index of 90PC/10PE was largely lower ($RIU_{fin} = 700 \mu$ RIU), compared to PC liposomes. All different liposome compounds were affected after rinsing by buffer solution (PBS).

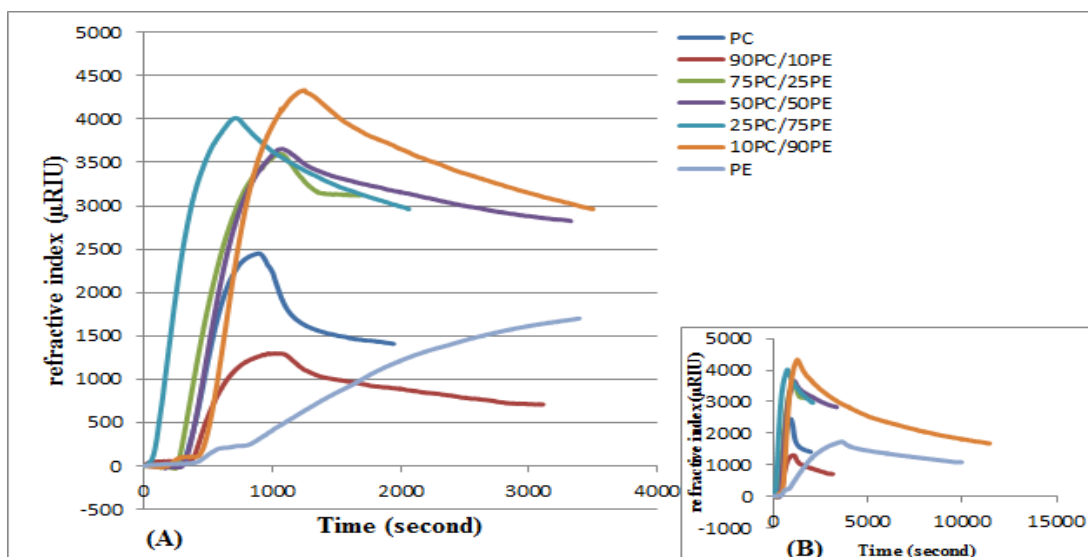


Figure 4.2: Change in SPR refractive index versus time for the interaction of PC and PC/PE liposomes onto the gold surface as a third layer. (A) shows RI changes up to 3500 seconds and (B) shows the results in an extended time frame.

High refractive index results obtained by PE concentrations between 25 and 75%, compared to PC liposomes showed that vesicle adsorption on the surface takes place very rapidly but fusion of liposomes on the surface to form a bilayer on our DSPE-PEG films was unsuccessful. High signal could be caused by multi-vesicle layer formation on the surface. Additionally, it can be seen from the figure 4.2B that further increase in PE concentration (10PC/90PE) affect the vesicle stability on the surface, and there was a slow and continuous decrease in RI during the washing step, which might indicate the loss of intact liposomes or water loss and bilayer formation on the surface. Lower PE concentrations (90PC/10PE) had a completely different behavior and it was comparable with that of pure PC liposomes. The reason for this behavior might be the differences in interactions between liposomes constituted from different lipid molecules, i.e. PC and PE: mixed liposomes might show higher interactions with each other and formed multiple liposome layers. The flexibility of the liposomes composed of different phospholipids is also different and rigidity also affect liposome fusion. The other parameter is the interaction of different phospholipids with the ions: PE lipid bilayers have been found to be influenced by monovalent salt to a significantly lesser extent compared to PC bilayers. As a consequence, PE lipids can form both intra- and intermolecular hydrogen bonds and hence adopt a more densely packed bilayer structure [46]. All these differences might contribute to the behavior difference of different liposomes.

Interpretation of SPR data was also complemented with QCM-D analysis. More information about the spreading of vesicles to form a tBLM can be obtained by measurements with the QCM-D. QCM-D allows the discrimination between a mere adsorption and the fusion of vesicles, as shown by Keller and Kasemo [5], by following the change in at least two parameters. Frequency change (Δf) is mainly related to the change in mass, whereas dissipation is related to changes in viscoelastic and rheological properties.

To determine adsorption behavior of PC/PE liposomes, PC liposomes was investigated at first. For a quantitative comparison of the lipid deposition process, the minimum in frequency, Δf_{\min} ($-68,8 \pm 15$ Hz), and the maximum in dissipation, ΔD_{\max} ($14,6 \pm 1 \times 10^{-6}$), were determined. Figure 4.3 demonstrates that after rinsing at a later stage, shortly after the minimum in frequency and the maximum in dissipation are reached, a considerable rearrangement of the surface-bound lipid material takes place within minutes. In the absence of vesicles in solution, Δf increased to -49 ± 9 Hz and ΔD decreased to $9 \pm 1 \times 10^{-6}$, indicating that the major part of adsorbed vesicular material was transformed into bilayer patches.

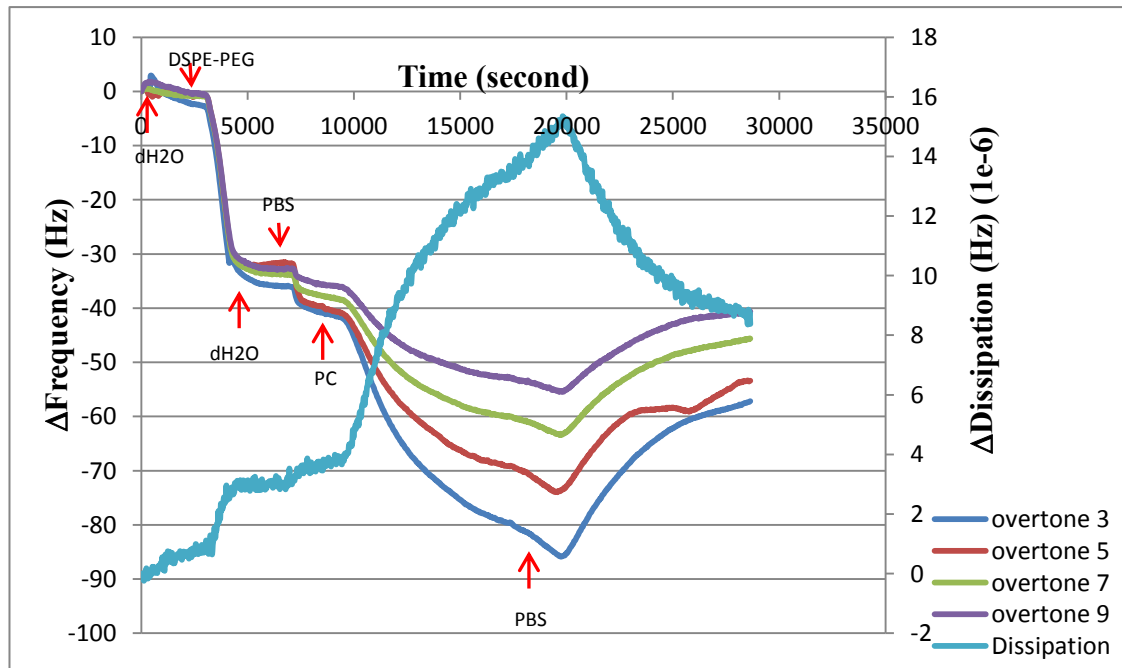


Figure 4.3: Change in QCM resonant (normalized) frequency and dissipation versus time for the interaction of PC liposomes onto the gold surface.

By using a QCM sensor, a distinct decrease of the frequency during the adsorption of vesicles was observed while the frequency decrease rapidly stopped in 3 hours in the case of vesicle fusion (Figure 4.4 and Figure 4.5).

Figure 4.4 shows QCM-D data for 75PC/25PE liposomes ($\Delta f_{\text{fin}} = 76.7 \pm 4.3 \text{ Hz}$, $\Delta D_{\text{fin}} = 12 \pm 1 \times 10^{-6} \text{ Hz}$, $\Delta D/\Delta f = 1.13 \pm 0.4$). Frequency and dissipation change of 75PC/25PE liposomes was slightly higher than PC liposomes. There was almost no change in frequency and a low decrease in dissipation values after rinsing. This could be majorly attributed to the adsorption of intact liposomes to the surface, and minimal vesicle loss from the during washing.

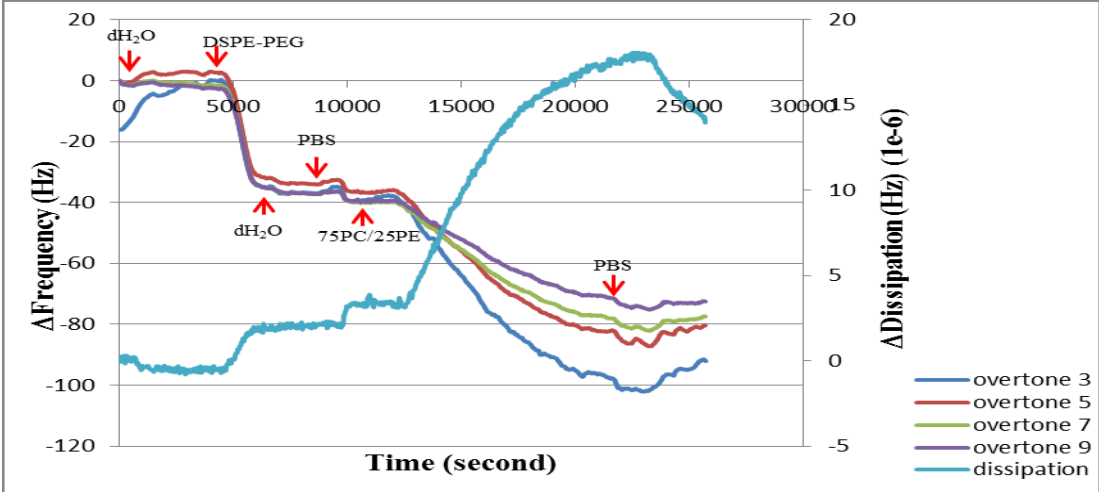


Figure 4.4: Change in QCM resonant (normalized) frequency and dissipation versus time for the interaction of 75PC/25PE liposomes onto the gold surface.

The adsorption of PE liposomes resulted in a frequency drop of about $-56.2 \pm 10 \text{ Hz}$ and in dissipation increase to $\sim 20 \pm 3 \times 10^{-6}$ (Figure 4.5). The $\Delta D/\Delta f$ value was calculated as $1.7 \pm 0.4 \text{ Hz}^{-1}$. The adsorption saturated at a value that was affected by rinsing. The increase in the Δf values after rinsing probably indicate that while major part of adsorbed vesicles remained intact, the minor part of adsorbed vesicular material was transformed into multilayer patches.

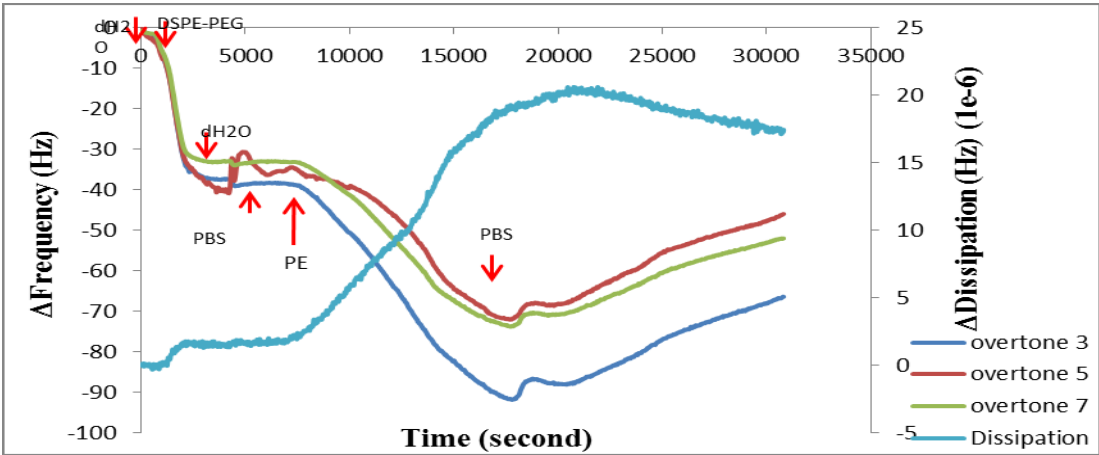


Figure 4.5: Change in QCM resonant (normalized) frequency and dissipation versus time for the interaction of PE liposomes onto the gold surface.

It is known that a high viscoelasticity of bound analytes induces an increase in dissipation. Moreover, $\Delta D/\Delta f$ slope offers a meaningful knowledge about liposome disruption and lipid bilayer generation [47]. Increasing $\Delta D/\Delta f$ ratio states high viscoelasticity of bound analytes [48]. In this case, $\Delta D/\Delta f$ value was increased by the addition of PE to PC liposomes. This increase shows that by adding more PE on liposomes, the membrane became more rigid as revealed by the decrease of the membrane fluidity. Since it is more difficult for membranes to fuse with each other for bilayer forming, the amount of remaining intact liposome could increase [49].

Moreover, PE is known to exhibit a higher headgroup hydration than PC, which should enhance a tighter packing of neighboring molecules [50]. The higher the headgroup hydration (PE), the deeper the molecules embed themselves in the water surface to the detriment of monolayer cohesion. Hence, PC headgroups induce better lateral intermolecular forces between phospholipids [51].

4.1.3 The effects of percentage of PS on PC/PS liposomes

The binding studies of anionic PC/PS liposomes prepared in different compositions shown in Table 3.1 was monitored in real-time on DTSP covered gold slides by SPR. The lipid concentration was 0.02 mg/ml. At least 2-3 experiments were performed to take data.

The Figure 4.6 shows a kinetic curve for surface plasmon optical recording. The change in reflected intensity monitored at a fixed angle of observation as a function of time rose by adding PS on liposomes. After rinsing, the end points of 90/10, 75/25, 50/50 and 10/90% of PC/PS liposomes indicated similarity and reached approximately the same refractive index level ($\sim 2400 \mu\text{RIU}$). 25PC/75PS liposomes was not affected after rinsing and reached to $3500 \mu\text{RIU}$.

PS liposomes showed markedly high refractive index result which is $3025 \mu\text{RIU}$. These refractive index values do not fit in with tBLMs formation results. Unfortunately, SPR results indicate that there was not tBLMs formation of anionic PC/PS and PS liposomes.

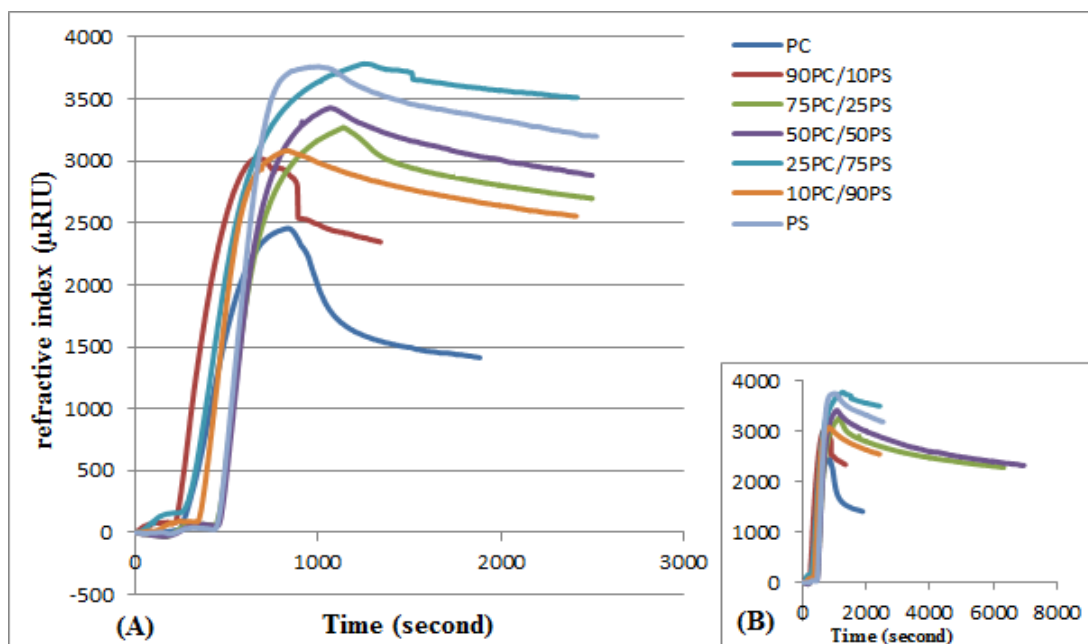


Figure 4.6: Change in SPR refractive index versus time for the interaction of PC and PC/PS liposomes onto the gold surface. (A) shows RI changes up to 2500 seconds and (B) shows the results in an extended time frame.

PC/PS liposomes adsorption kinetic showed very similar adsorption-desorption kinetics in SPR results. When the QCM results for these liposomes were examined (later in the section), it could be seen that both ΔD and Δf values were at least twice fold more compared with PC/PE liposomes so multiple layers were probably formed on the surface and this caused a thicker layer. The similarities in the results might be caused by SPR exponential decay. The evanescent field determines the size of macromolecules or particles which can be studied, as it is enhanced near the surface and decays exponentially with distance away from it (Figure 4.7) [52].

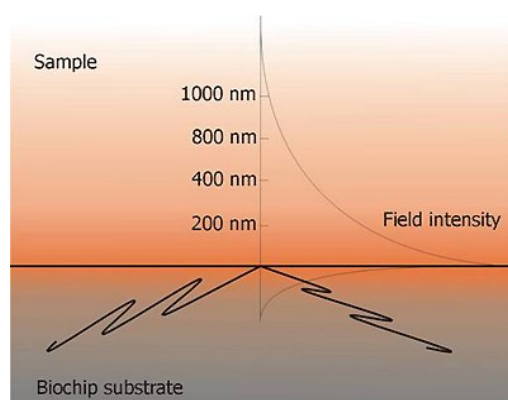


Figure 4.7: The evanescent field of SPR.

According to Figure 4.7, a thickness of 100 nm or below from the surface is ideal for the studies, so when vesicles adsorbed as multilayers larger than that, the signal is not linear and it would not reflect the amount of bound vesicles. Therefore, in our study, multilayer vesicle adsorption might not be detected very efficiently by SPR and because of this, the results from QCM-D technique was used to interpret the surface characteristics.

According to the QCM-D results, the frequency change was 159 ± 40 Hz and the maximum dissipation shift for 75PC/25PS liposomes, $\Delta D_{\max} = 42 \times 10^{-6}$, was remarkably high, resulting in a ratio between dissipation and frequency of $\Delta D_{\max} / \Delta f_{\min} = 2 \pm 1.5 \times 10^{-6} \text{ Hz}^{-1}$ (Figure 4.8). This was significantly more than bilayer formation of PC liposomes ($1.2 \pm 0.6 \times 10^{-6} \text{ Hz}^{-1}$). ΔD allows distinguishing between the viscoelastic state of the adsorbed lipids: intact vesicles exhibit high dissipation while bilayer (patches) show low dissipation [1]. After obtaining the plateau, a rinse was performed and no change in frequency or dissipation was observed. Therefore, these results represent the presence of intact multi-PC/PS liposomes layer on the surface.

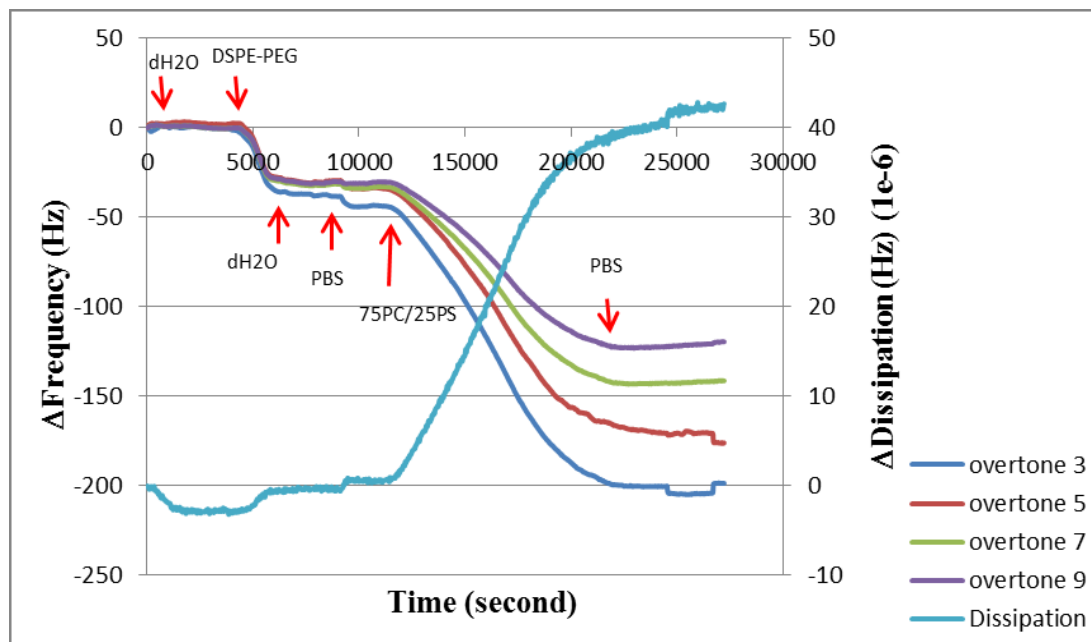


Figure 4.8: Change in QCM resonant frequency (normalized) and dissipation versus time for the interaction of 75PC/25PS liposomes onto the gold surface.

Figure 4.9 illustrates the respective parameters during adsorption of vesicles of PS on a DSPE-PEG monolayer. The binding process, which corresponds to an decrease of -180.5 ± 38.5 in frequency change (normalized) and an increase about 37.5×10^{-6} in

dissipation, was complete within 10 hours. $\Delta D/\Delta f$ value was calculated as $1.5 \pm 1 \text{ Hz}^{-1}$. The adsorption of vesicles was not affected by rinsing. The lack of an abrupt frequency (mass) or dissipation (rigidity) change, also high Δf and ΔD values indicate that the vesicles are stable, formed multi-vesicle layer and well adsorbed to the surface [21].

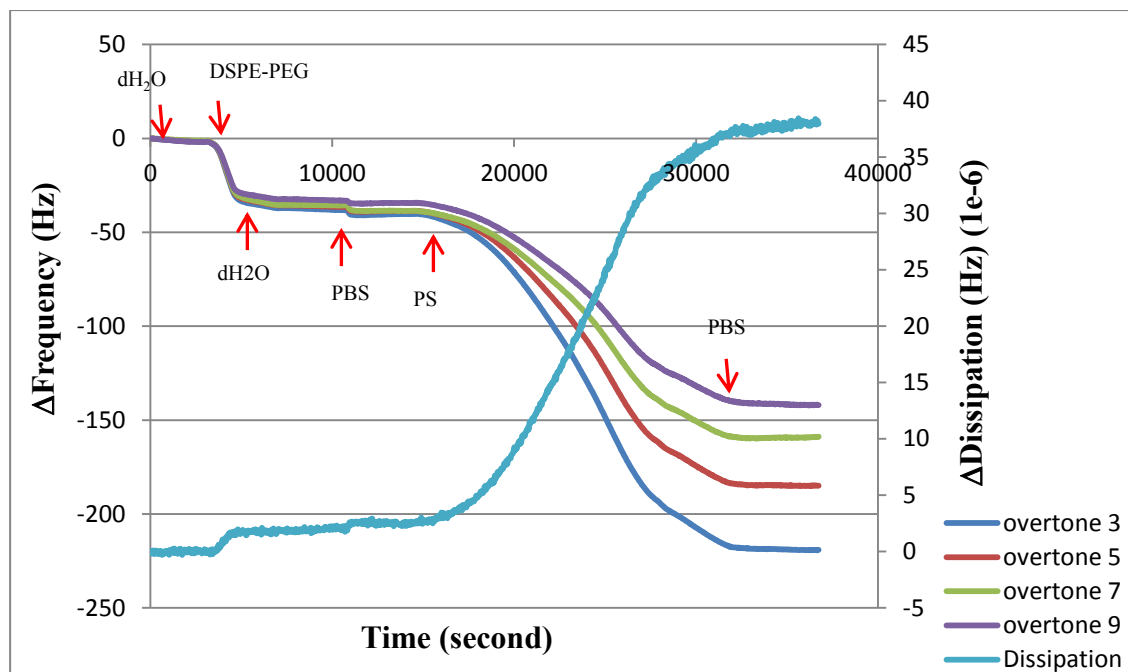


Figure 4.9: Change in QCM resonant frequency (normalized) and dissipation versus time for the interaction of PS liposomes onto the gold surface.

Frequency and dissipation changes reported in the literature are considerably high and differ from our studies. For example, in the study of Richter [1], lipid deposition pathways measured by QCM-D on silica and supported lipid bilayer formation was observed. 50DOPC/50DOPS liposomes have caused a decrease of -50 Hz in frequency and an increase of $2.5 \times 10^{-6} \text{ Hz}^{-1}$ in dissipation which indicate intact vesicle adsorption on the silica surface. However, both the swollen DSPE-PEG layer and the large vesicles are highly viscoelastic, the dissipation of energy should be much higher than these systems. Moreover, the vesicle deposition in buffer exhibits a high dissipation [53].

There might not be a strong enough driving force for the vesicles to spread on these PEG films under PBS. Therefore, to induce lipid bilayer formation of 25PC/75PS liposomes and to check their stability, 70% ethanol solution was used (Figure 4.10). After rinsing with ethanol, a rapid decrease in refractive index was observed. When the system reached a plateau, buffer solution (PBS) was passed through the surface

to observe whether the system is stable or not. However, the refractive index continued to decrease to the previous value (1000 μ RIU), which indicates the DSPE-PEG surface. In this case, the lipid molecules could not stay stable on the surface.

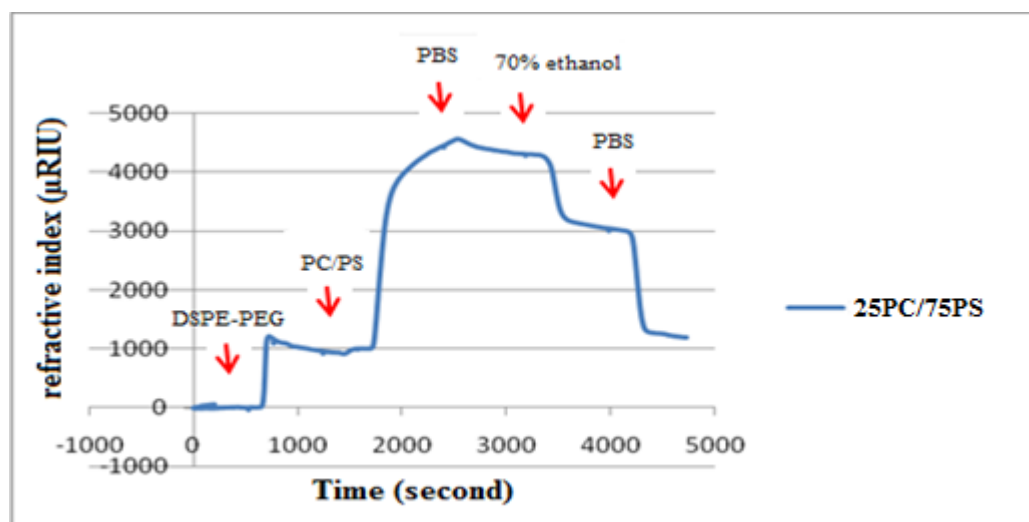


Figure 4.10: SPR sensogram of 25PC/75PS liposomes rinsed by 70% of ethanol solution.

In the literature, there are other methods to create lipid bilayers on solid substrates. One of these methods was inspired from “painting method” in which lipids are deposited onto hydrophobic surfaces from ethanol or an alkane solvent, such as hexane or decane, and then exposed to water [54]. To reduce the surface energy that arises from the interactions of the hydrophobic surface with water, the free lipids self-assemble into an upper leaflet where the hydrophilic headgroups are exposed to the water. In the study of Jeffrey C. Munro [29], they attempted to use a similar driving force to deposit the bottom lipid leaflet. They have demonstrated that bilayer regions on the DSPE-PEG-PDP films can be created with a range of tethered lipid densities from 0.1 to 6 mol % by using this method. After chemisorption of the PEG films to the gold surface, egg-PC lipids were physisorbed on the PEG films from a hexane solution. Finally, vesicles were adsorbed and fused to the sample in an aqueous environment, resulting in tethered lipid bilayers. However, fluorescence microscopy and electrochemical impedance spectroscopy measurements have shown that the physisorbed lipid films deposited from the hexane solution are poorly organized, and the mechanism of bilayer formation during the subsequent vesicle fusion step is not fully understood [29].

4.2 Effect of Liposome Size

In order to confirm whether liposomes size is important for the adsorption process on this modified surface electrode, 90PC/10PE and 75PC/25PE liposomes were prepared with a 50 nm membrane filter instead of 100 nm. As can be seen in Figure 4.11, decreasing the liposome size to 50 nm had negative effect on the adsorption behavior of the liposomes on the surface. Even without rinsing the surface by PBS, the adsorbed vesicles started to detach from the surface and the refractive index continued to decrease to its previous value of 1500 μ RIU, which indicates the DSPE-PEG surface. This indicated that the vesicles could not interact with DSPE-PEG layer and/or with each others efficiently to form a stable layer on the surface.

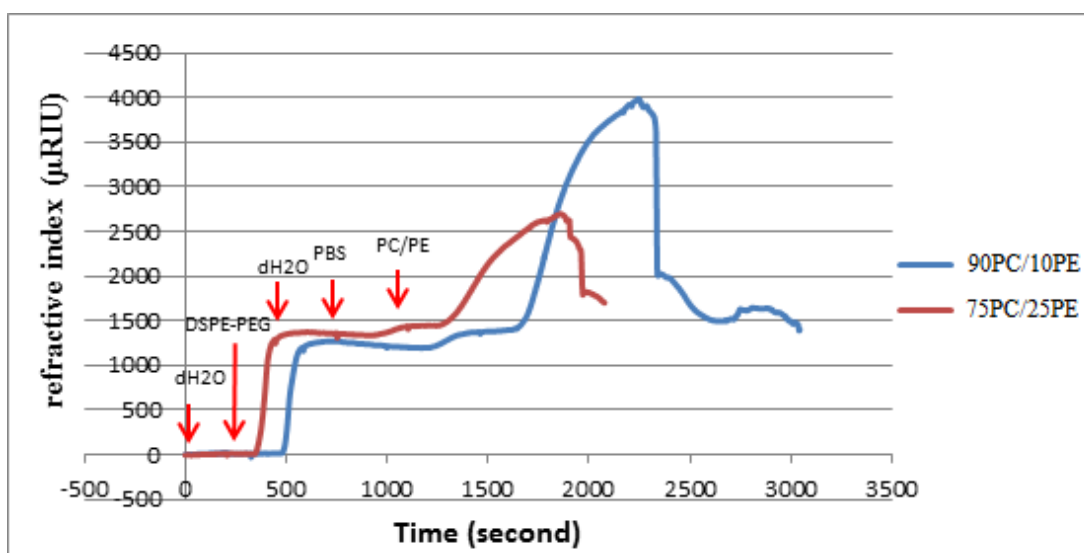


Figure 4.11: Change in SPR refractive index versus time for the interaction of PC/PE liposomes, which are formed by 50nm membrane, onto the gold surface.

5. CONCLUSIONS AND RECOMMENDATIONS

Tethered bilayer lipid membranes (tBLMs) are important development that provides the biomimesis of lipid bilayer membranes. tBLMs also allow for the application of a variety of surface analytical techniques.

In this study, the effect of liposomes with different phospholipids and different compositions on tBLMs formation was evaluated with SPR and QCM-D. Complemented results of SPR and QCM-D provide magnitude information about adsorption properties of liposomes by the help of refractive index and frequency (Δf) and dissipation (ΔD) change values, respectively. Additionally, change in $\Delta D/\Delta f$ slope provides to determine viscoelastic properties of formed bilayer or vesicles on the surface.

According to the SPR and QCM-D results, presence of either PE or PS on liposome composition affects tBLMs formation on the surface. PE had an effect on fluidity of PC liposomes. While adding PE on PC liposomes, the membrane became more rigid, it is more difficult for membranes to fuse with each other for bilayer formation, and this causes that the amount of remaining intact vesicle increase.

By adding PS on PC liposomes, a significant increase in refractive index and dissipation indicates multi-vesicle layer formation on the surface. Moreover, rinsing the surface by 70% of ethanol after adsorption of 25PC/75PS liposomes was unsuccessful to rupture vesicles and induce bilayer formation.

Besides all these, the effect of vesicle size was also investigated. Liposomes prepared with a 50 nm diameter membrane filter instead of 100 nm was shown to be washed off easily from the surface without forming a bilayer.

Information about the adsorbed material obtained by QCM-D and SPR measurements can be insufficient to determine a small fraction of prematurely ruptured vesicles [53]. Therefore, complementing studies like liquid atomic force microscopy (AFM) may be performed to provide direct evidence that gold surface can be covered with vesicles or bilayer patches.

In conclusion, the phospholipid content of liposomes has a great impact on the behavior of liposomes and different parameters like the size, fluidity and interaction with different ions affect this behavior. Since the cell membrane of different tissues have different compositions, these parameters should be investigated in more detail.

REFERENCES

- [1] **Richter, R. P., Berat, R., and Brisson, A.** (2003). Formation of Solid-Supported Lipid Bilayers: An Integrated View, *Langmuir*, **22**, pp. 3497-3505.
- [2] **Rossi, C., Chopineau, J.** (2007). Biomimetic tethered lipid membranes designed for membrane-protein interaction studies, *Eur Biophys J*, **36**, p. 955–965.
- [3] **Richter, R. P., Him, J. L. and Brisson, A.** (2003). Supported Lipid membranes, *Materials Today*, pp. Laboratory of Molecular Imaging and NanoBioTechnology, IECB, CNRS-UMR 5471.
- [4] **Giess, F., Friedrich, M. G., Heberle, J., Naumann, R. L., and Knoll, W.** (2004). The Protein-Tethered Lipid Bilayer: A Novel Mimic of the Biological Membrane, *Biophysical Journal*, **87**, p. 3213–3220.
- [5] **Keller, C. A., Kasemo, B.** (1998). Surface Specific Kinetics of Lipid Vesicle Adsorption Measured with a Quartz Crystal Microbalance, *Biophys. J.*, **75**, p. 1397–1402.
- [6] **Alves, I. D., Park, C. K., and Hruby, V. J.** (2005). Plasmon Resonance Methods in GPCR Signaling and Other Membrane Events, *Curr Protein Pept Sci.*, **6**, p. 293–312,
- [7] **Vockenroth, I. K., Rossi, C., Shah, M. R., and Köper, I.** (2009). Formation of tethered bilayer lipid membranes probed by various surface sensitive techniques, *Biointerphases*, **4**, pp. 19-26.
- [8] **Junghans, A., and Köper, I.** (2010). Structural Analysis of Tethered Bilayer Lipid Membranes, *Langmuir*, **26**, pp. 11035-11040.
- [9] **Volker, K., Marta, K., David, M., Chen, W., and Lukas, K.** (2008). Supported Lipid Bilayers: Development and Applications in Chemical Biology, *Wiley Encyclopedia Of Chemical Biology*.
- [10] **Yip, S.H.** (2007). Supercritical Fluid Extraction and Chromatography of Various Lipids from Soybean Lecithin, *Master's Thesis at Virginia Tech.*, Date retrieved: 02.03.2012, adress: <http://scholar.lib.vt.edu/theses/available/etd-10102007-145321/>
- [11] **Srivastava, M.** (2010). High Performance Thin-Layer Chromatography (HPTLC), *Springer*.
- [12] **Alberts, B., Johnson, A., Lewis, J.** (2002). Molecular Biology of the Cell. *4th edition*, New York: Garland Science.
- [13] **Taylor, C.** (2002). Controlling calcium entry, *Cell*, **111**, pp. 767-769.
- [14] **Uran, S., Larsen, A., Jacobsen, P. B., and Skotland, T.** (2001). Analysis of phospholipid species in human blood using normal-phase liquid

chromatography coupled with electrospray ionization ion-trap tandem mass spectrometry, *J. Chromatogr. B*, **758**, pp. 265-275.

- [15] **Vance, J. E.** (2008). Phosphatidylserine and phosphatidylethanolamine in mammalian cells: two metabolically related aminophospholipids, *Journal of Lipid Research*, **49**.
- [16] **Post, J. A., Bijvelt, J. J., and Verkleij, A. J.** (1995). Phosphatidylethanolamine and sarcolemmal damage during ischemia or metabolic inhibition of heart myocytes, *Am. J. Physiol*, **268**, pp. H773-H780.
- [17] **Emoto, K., Toyamasorimachi, N., Karasuyama, H., Inoue, K., and Umeda, M.** (1997). Exposure of phosphatidylethanolamine on the surface of apoptotic cells, *Exp. Cell Res.*, **232**, pp. 430-434.
- [18] **Daleke, D.** (2007). Phospholipid flippases, *J Biol Chem.* , **282**, pp. 821-825.
- [19] **Fang, Y.** (2011). Air stability of supported lipid membrane spots, *Chemical Physics Letters*, **512**, no. 4-6, pp. 258-262.
- [20] **Chan, Y. M., and Boxer, S. G.** (2007). Model Membrane Systems and Their Applications, *Current Opinion in Chemical Biology*, **11**, pp. 581-587.
- [21] **Dorvel, B. R., Keizer, H. M., Fine, D.** (2007). Formation of Tethered Bilayer Lipid Membranes on Gold Surfaces: QCM-Z and AFM Study,» *Langmuir*, **23**, pp. 7344-7355.
- [22] **Vecer, J., Herman, P., and Holoubek, A.** (1997). Diffusion membrane potential in liposomes: setting by ion gradients, absolute calibration and monitoring of fast changes by spectral shifts of Dis-C-3(3) fluorescence maximum, *Biochim. Biophys. Acta.*, **1325**, pp. 155-164.
- [23] **Cremer, P. S., and Boxer, S. G.** (1999). Formation and Spreading of Lipid Bilayers on Planar Glass Supports, *J. Phys. Chem. B.*, **103**, p. 2554.
- [24] **Knoll, W., Frank, C. W., Heibe, C. I., Naumann, R., Offenhausser, A., Ruhe, J., Schmidt, E. K., Shen, W. W., and Sinner, A.** (2000). Functional Tethered Lipid Bilayers, *J. Biotechnol.*, **74**, pp. 137-158.
- [25] **Krishna, G., Schulte, J., Cornell, B. A., Pace, R. J., and Osman, P. D.** (2003). Tethered Bilayer Membranes Containing Ionic Reservoirs: Selectivity and Conductance, *Langmuir*, **19**, pp. 2294-2305.
- [26] **Naumann, R., Schiller, S. M., Giess, F., Grohe, B., Hartman, K. B., Karcher, I., Koper, I., Lubben, J., Vasilev, K., and Knoll, W.** (2003). Tethered Lipid Bilayers on Ultraflat Gold Surfaces, *Langmuir*, **19**, pp. 5435-5443.
- [27] **Bally, M., Bailey, K., Sugihara, K., Grieshaber, D., Vörös, J.** (2010). Liposome and Lipid Bilayer Arrays Towards Biosensing Applications, *Small* , pp. 2481-2497.
- [28] **Harris, J. M.** (1992). Poly(Ethylene Glycol) Chemistry: Biotechnical and Biomedical Applications, Katritzky, A. R., Sabongi, G. J., Eds.; Plenum Press: New York.

- [29] **Munro, J. C., and Frank, C. W.** (2004). Adsorption of Lipid-Functionalized Poly(ethylene glycol) to Gold Surfaces as a Cushion for Polymer-Supported Lipid Bilayers, *Langmuir*, **20**, pp. 3339-3349.
- [30] **Homola, J.** (2008). Surface plasmon resonance sensors for detection of chemical and biological species, *Chem Rev.*, **108**, no. 2, p. 462–493.
- [31] **Scarano, S., Mascini, M., Turner, A. P. F., Minunni, M.** (2010). Surface plasmon resonance imaging for affinity-based biosensors, *Biosens Bioelectron*, **25**, no. 5, p. 957–966.
- [32] **Merwe, P. A.** (n.d). Surface Plasmon Resonance, Date retrieved: 10.03.2012, adress: <http://users.path.ox.ac.uk/~vdmerwe/internal/spr.pdf>
- [33] **Liu, X., Song, D., Zhang, Q., Tian, Y., Ding, L., Zhang, H.** (2005). Wavelength-modulation Surface Plasmon Resonance Sensor, *Trends in Analytical Chemistry*, **24**.
- [34] **Wijaya, E., Lenaerts, C., Maricot, S., Hastanin, J., Habraken, S., Vilcot, J. P.** (2011). Surface plasmon resonance-based biosensors: From the development of different SPR structures to novel surface functionalization strategies, *Current Opinion in Solid State and Materials Science*, **15**, pp. 208-224.
- [35] **Otto, A.** (1968). Excitation of Nonradiative Surface Plasma Waves in Silver by the Method of Frustrated Total Reflection,» *Z. Phys.*, **216**, p. 398.
- [36] **KSV Ltd.** (2004). What is a Quartz Crystal Microbalance – QCM.
- [37] **Kanazawa, K., and Nam-Joon, C.** (2009). Quartz Crystal Microbalance as a Sensor to Characterize Macromolecular Assembly Dynamics, *Journal of Sensors*.
- [38] **Garg, R.** (2008). Extreme Ultraviolet Resist Outgassing and Its Effect on Nearby Optics, College of Nanoscale Science and Engineering.
- [39] **Nirschl, M., Reuter, F., and Vörös, J.** (2011). Review of Transducer Principles for Label-Free Biomolecular Interaction Analysis, *Biosensors* , **1**, pp. 70-92.
- [40] **Cho, N. J., Kanazawa, K. K., Glenn, J. S., and Frank, C. W.** (2007). Employing Two Different Quartz Crystal Microbalance Models To Study Changes in Viscoelastic Behavior upon Transformation of Lipid Vesicles to a Bilayer on a Gold Surface, *Anal. Chem.*, **79**, pp. 7027-7035.
- [41] **Matthew, A., and Victoria, T.** (2007). A Survey of the 2001 to 2005 quartz crystal microbalance biosensor literature: applications of acoustic physics to analysis of biomolecular interactions, *Journal of Molecular Recognition*, **20**, no. 3, pp. 154-184.
- [42] **Dixon, M. C.** (2008). Quartz Crystal Microbalance with Dissipation Monitoring: Enabling Real-Time Characterization of Biological Materials and Their Interactions, *Journal of Biomolecular Techniques*, **19**, pp. 151-158.

- [43] **Kanazawa, K., and Gordon, J.G.** (1985). The Oscillation Frequency of a Quartz Resonator in Contact with a Liquid, *Anal. Chim. Acta*, **175**, pp. 99-105.
- [44] **Knoll, W., Koper, I., Naumann, R., Sinner, E. K.** (2008). Tethered bimolecular lipid membranes: A novel model membrane platform, *Electrochimica Acta*, **53**, pp. 6680-6689.
- [45] **Kök, F. N.** (project manager) (2011). Bir Zar Proteini Olan P-Glikoproteininin Yapay Lipit Zarlara Yerleştirilmesi ve Statin Bazlı Kolesterol Düşürücü İlaçlarla Etkileşimi, *TUBITAK Project, Project number: 108T933*.
- [46] **Gurtovenko, A. A., and Vattulainen, I.** (2008). Effect of NaCl and KCl on Phosphatidylcholine and Phosphatidylethanolamine Lipid Membranes: Insight from Atomic-Scale Simulations for Understanding Salt-Induced Effects in the Plasma Membrane, *Journal of Physical Chemistry B*, **112**, p. 1953-1962.
- [47] **Bendas, D.** (2010). Biosensor-Based Evaluation of Liposomal Binding Behavior, Liposomes: Methods and Protocols, *Biological Membrane Models*, ed: V. Weissig, Humana Press, **2**, p. 519.
- [48] **Höpfner, M., Rothe, U., Bendas, G.,** (2008). Biosensor-Based Evaluation of Liposomal Behavior in the Target Binding Process, *Journal of Liposome Research*, **18**, pp. 71-82.
- [49] **Vu, T. H., Shimanouchi, T., Ishii, H., Umakoshi, H., Kuboi, R.** (2009). Immobilization of intact liposomes on solid surfaces: A quartz crystal microbalance study, *Journal of Colloid and Interface Science*, **336**, p. 902–907.
- [50] **Pimthon, J., Willumeit, R., Lendlein, A., Hofmann, D. J.** (2009). Membrane association and selectivity of the antimicrobial peptide NK-2: a molecular dynamics simulation study, *Pept. Sci.*, **15**, pp. 654-657.
- [51] **Anton, N., Saulnier, P., Boury, F., Foussard, F., Benoit, J. P. and Proust, J. E.** (2007). The influence of headgroup structure and fatty acyl chain saturation of phospholipids on monolayer behavior: a comparative rheological study, *Chem. Phys. Lipids*, **150**, p. 167–175.
- [52] **Url-1** < <http://www.xantec.com/new/index.php?content=11>>, date retrieved 02.05.2012.
- [53] **Reimhult, E., Hook, F. and Kasemo, B.** (2002). Vesicle adsorption on SiO₂ and TiO₂: Dependence on vesicle size, *J. Chem. Phys.*, **117**, p. 7401.
- [54] **Florin, E. L., Gaub, H. E.** (1993). Painted supported lipid membranes. *Biophys. J.*, **64**, p. 375-383.

APPENDICES

APPENDIX A: Laboratory Equipments

APPENDIX B: Chemicals & Buffers

APPENDIX A

Laboratory Equipment

Pipettes (Eppendorf 10 µl, 100 µl, 1000 µl, 2500 µl, 5000 µl)

pH meter (Hanna Instruments, HI 9124)

Magnetic stirrer (Cole-Parmer, Stable Temp)

Bath Sonicator (Transsonic TP 690)

Vortex (Heidolph, REAX top)

SPR (Reichert SR7000)

QCM-Z500 (KSV Instruments)

Tubing (Tygon, SC0060; R3607)

Peristaltic pump

Filter Support (10mm Filter Supports, 610014 Avanti Polar)

PC Membranes (0.1 µm Polycarbonate Membranes, 610005 Avanti Polar)

QCM slides (Q-Sense, Sweden)

SPR slides

Mini-Extruder (Avanti Polar Lipids/Hamilton Company, 610017)

Extruder membranes (Whatman, Nuclepore Track-Etch Membrane 0.1 µm, 800309)

APPENDIX B

Chemicals

PC (Sigma-Aldrich)

PE (Avanti Polar Lipids)

PS (Avanti Polar Lipids)

PBS (Phosphate buffered saline)

- 1.78 g $\text{Na}_2\text{HPO}_4 \cdot 2\text{H}_2\text{O}$
- 0.27 g KH_2PO_4
- 0.20 g KCl
- 8 g NaCl in 1 liter
- Adjust pH 7.4 with HCl or NaOH

Ethanol (Sigma, 32221-SL)

Isopropanol (Sigma, 24137)

Sodium Chloride

Potassium Chloride

Sodium Hydroxide

Hydrochloric Acid

Potassium Dihydrogenphosphate (KH_2PO_4)

Disodium Hydrogen Phosphate Dihydrate ($\text{Na}_2\text{HPO}_4 \cdot 2\text{H}_2\text{O}$)

Chloroform

SDS (sodium dodecyl sulfate)

CURRICULUM VITAE



Name Surname: Başak TÜRKEN

Place and Date of Birth: Edirne, 08.07.1987

Address: Kuvayi Milliye Cad., Şendeniz Apt, no: 17 Fatih/İstanbul

E-Mail: basakturken@gmail.com

B.Sc.: Molecular Biology and Genetics, Istanbul University (2005-2009)

List of Publications and Patents:

- Gunel T., Kalelioglu I., Surmeli Y., **Turken B.**, Ermis H., and Aydınli K.,: Comparison of Real-time Polymerase Chain Reaction Assay Methods for Detection of RHD Gene in Amniotic Fluid, *J. Nat. Sci. Biol. Med.*, 2011, Jul-Dec; 2(2): 193–197.

PUBLICATIONS/PRESENTATIONS ON THE THESIS

- **Turken, B.**, Inci F., Kok F.N., 2011: The Effect of Liposome Phospholipid Content on The Formation of Tethered Bilayer Lipid Membranes. *36thThe Federation of European Biochemical Societies Congress*, June 25-30, 2011 Torino, Italy.
- **Turken, B.**, Kok F.N., 2012: The Effect of Liposome Phospholipid Content on The Formation of Tethered Bilayer Lipid Membranes. *8thNanoscience and Nanotechnology Congress*, June 25-29, 2012, Ankara, Turkey.